Specifying non-white light sources in outdoor applications to reduce light pollution

Tony Esposito, PhD[1]
Leora C. Radetsky, MS, LC[2]*

[1]Lighting Research Solutions LLC
[2]DesignLights Consortium

Abstract

Anthropogenic ("human-generated") light at night (ALAN) from outdoor lighting produces light pollution and as a result causes a range of deleterious responses in humans, plants, and animals. An emerging strategy to combat light pollution, especially sky glow, is to use "amber" LEDs in lieu of phosphor-converted white LEDs with high correlated color temperatures. Importantly, however, there is no standardized terminology or chromaticity designation that is applicable to "amber" LED lighting products for outdoor illumination. In this work, we propose a specification structure for light sources with non-standard chromaticities to increase the precision of language used in the architectural lighting industry and demonstrate that light sources with well-defined chromaticity ranges outside of the ANSI C78.377-2017 quadrangles may be useful for reducing the portion of relative sky glow related to light source spectral power distribution. We encourage lighting standards development organizations to consider standardizing such a system.

Keywords: amber, anthropogenic light at night (ALAN), artificial light at night, light pollution, light emitting diodes, architectural lighting, sky glow

*Corresponding author: lradetsky@designlights.org

This is an Accepted Manuscript of an article published by Taylor & Francis in LEUKOS on January 5, 2023, available at: https://www.tandfonline.com/doi/full/10.1080/15502724.2022.2121285

1. Introduction

Sky glow is a form of light pollution described by "the brightening of the night sky that results from the scattering and reflection of light from the constituents of the atmosphere [of Earth]…in the direction of the observer" (IES 2021a). All anthropogenic ("human generated") sources of light at night (ALAN) that allow direct and reflected scattering of light into the open air contribute to sky glow, among them, in no particular order, are: sports field lighting, advertising signage, media screens, façade lighting, street lighting, car headlights, light leak from residential and commercial buildings, greenhouse lighting, oil-well flares, fishing lights, and lighting on offshore drilling rigs.

ALAN limits or eliminates the view of the sky from Earth and poses potential threats to plants and animals, scientific research, professional and amateur astronomical observations, and wastes a significant amount of energy at great environmental and financial cost.

This wasted light is estimated to cost the United States at least USD $7 Billion yearly, generating nearly 66 million metric tons of CO_2, the equivalent of 9.5 million cars (Gallaway et al. 2010). Most humans now experience light-polluted night skies. Cinzano et al. (2001) and Falchi et al. (2016), respectively, illustrate the severity of the problem:

> "About two-thirds of the World population and 99 per cent of the population in the United States (excluding Alaska and Hawaii) and European Union live in areas where the night sky is above the threshold set for polluted status. Assuming average eye functionality, about one-fifth of the World population, more than two-thirds of the United States population and more than one half of the European Union population have already lost naked eye visibility of the MilkyWay."

> "…more than 80% of the world and more than 99% of the U.S. and European populations live under light-polluted skies. The Milky Way is hidden from more than one-third of humanity, including 60% of Europeans and nearly 80% of North Americans. Moreover, 23% of the world's land surfaces between 75°N and 60°S, 88% of Europe, and almost half of the United States experience light polluted nights."

To add insult to injury, the problem is getting worse. Kyba et al. (2017) estimate that across the globe both lit area and radiance of light area is increasing by approximately 2.2% per year, which is likely an underestimate since the satellite used to measure radiance has no sensitivity below 500 nm, a portion of the spectrum where LED lighting has more radiation than incumbent sources such as low-pressure sodium (LPS) and high-pressure sodium (HPS). Recent estimates of the hidden impact of the transition to LEDs postulate an upward radiance increase between 1992 and 2017 as high as 270% globally and 400% in some regions (Sánchez de Miguel et al. 2021).

It is also expected that global demand for light has not been saturated (Tsao and Waide 2013). This is potentially problematic since increases in energy efficiency and decreases in the cost of light generation may result in more per-capita light output, not less. This is a rebound effect (Birol and Keppler 2000) commonly known as the Jevons Paradox (Alcott 2005).

Without serious intervention ALAN will increase, increasing light pollution, sky glow, and a suite of deleterious impacts on humans (Cao et al. 2023) and wildlife (Sanders et al. 2021). ALAN is not only a disruptor to our view of the night sky (Aubé et al. 2018) and to biodiverse organisms and systems (Rich and Longcore 2006; Davies et al. 2012; Grubisic et al. 2019; Owens et al. 2020; Lewis et al. 2020; Kühne et al. 2021), the wasted energy is an impediment to humanity's decarbonization goals.

One strategy to reduce sky glow from ALAN is to limit short-wavelength energy from outdoor electric light sources (CIE 1997; Falchi et al. 2011; Aubé et al. 2013; Luginbuhl et al. 2014; Kinzey et al. 2017; Hartley and Liebel 2020), since particles in the atmosphere more strongly scatter short wavelength radiation than long wavelength radiation (referred to as Rayleigh and Mie scattering).

This is an Accepted Manuscript of an article published by Taylor & Francis in LEUKOS on 01/05/2022, available online: https://www.tandfonline.com/doi/full/10.1080/15502724.2022.2121285

Incumbent street lighting technology such as quasi-monochromatic low-pressure sodium (LPS) lamps and nearly orange high-pressure sodium (HPS) contain relatively low short-wavelength energy. Modern LED streetlights have, on average, proportionally more short-wavelength radiation, especially those with high correlated color temperatures (CCTs) marketed as "energy efficient". One potential strategy for reducing relative sky glow and other negative impacts of ALAN is to move towards, not away from, antiquity by limiting the amount of short-wavelength radiation present in a light sources spectral power distribution (SPD). One popular emerging strategy is to use outdoor LED luminaires with "amber" LED sources.

In this work we seek to explore the extent to which limiting short-wavelength radiation in a light source's SPD reduces relative sky glow and if commercial non-white LED technologies play an important role in this effort.

1.2. Background

Solid-state lighting (SSL) products emitting white light are typically described by their categorical correlated color temperature (CCT) derived from standardized chromaticity boundaries. These standardized chromaticity boundaries are defined by the American National Standards Institute (ANSI)/National Electrical Manufacturers Association (NEMA) C78.377-2017 (NEMA 2017). The standard provides a unified method to determine the categorical CCT of white light sources based on the inclusion of a light source's chromaticity in defined quadrangles (henceforth referred to as the "ANSI quadrangles") which generally take the form of parallelograms. The 10 CCT categories are 2200, 2500, 2700, 3000, 3500, 4000, 4500, 5000, 5700, and 6500 K. No chromaticities below 2136 K—the lower limit of the 2200 K quadrangle—have a defined CCT designation.

The *Basic* ANSI quadrangles are approximately centered on the Planckian locus with tolerances of either 7-step or 4-step MacAdam Ellipses (MacAdam 1942; MacAdam 1943; MacAdam 1985). The *Extended* quadrangles are located below the *Basic* quadrangles and were developed based on research showing that chromaticities in this range appear more "neutral" or more "natural" (see Annex E of ANSI/NEMA C78.377-2017 (NEMA 2017). The ANSI quadrangles are intended for light sources used in indoor general lighting applications, though they are commonly used for outdoor lighting luminaires too.

Because the ANSI quadrangles are used to define the chromaticity boundaries of what is typically considered "white" light, we will refer to chromaticities outside of these designations as "non-white" light (NWL). In this work we will be specifically concerned with chromaticities outside of the ANSI quadrangles in the direction of lower CCT which have, on average, proportionally less short wavelength radiation.

Common sources of non-white light in the outdoor nighttime environment include the following:

- Low pressure sodium (LPS): A discharge lamp in which light is produced by radiation from sodium vapor operating at a partial pressure of 0.1 Pa to 1.5 Pa (approximately 10-3 to 10-2 Torr). (IES 2021a). LPS lamps are notable for their saturated orange/amber color appearance, high luminous efficacy, near monochromatic spectral emission, and nearly zero ability to render colors.

- High pressure sodium (HPS): A high intensity discharge (HID) lamp in which light is produced by radiation from sodium vapor operating at a partial pressure of about 1.33 x 104 Pa (100 Torr) (IES 2021a). HPS lamps are notable for their orange color appearance, poor color rendition, and high luminous efficacy.

- Phosphor-converted amber LED ("PC Amber"): A PC Amber LED is based on a blue-emitting Indium Nitride-Gallium Nitride chip (InGan) paired with a reddish phosphor that fully, or nearly fully, down-converts the short wavelength radiation into longer wavelength broadband emission with a peak wavelength occurring near approximately 595 nm to 605 nm, and a full-width at half-maximum (FWHM) range of 80 nm to 90 nm (Mueller-Mach et al. 2009).

- Direct-emission amber LED ("DE Amber"): A DE Amber LED is based on an Aluminum-Indium-Gallium-Phosphide chip (AlInGaP) directly emitting long wavelength radiation with a peak wavelength of 590 nm to 605 nm, and a FWHM of approximate 15 nm to 20 nm.

- Phosphor-converted non-white LEDs (e.g., "PC 2000 K"): A PC non-white LED is based on a blue-emitting Indium Nitride-Gallium Nitride chip (InGan) paired with a reddish phosphor that partially down converts the short wavelength radiation into longer wavelength broadband emission with a peak wavelength occurring around 610 nm, and a FWHM ranging from approximate 80 nm to 90 nm. The chromaticity coordinates of these LED light sources lie near the Planckian locus with target CCTs lower than approximately 2200 K.

- Other direct-emission narrowband LEDs (e.g., "DE Red"): These non-white LEDs, such as direct emitting AlInGaP red LEDs, emit narrowband radiation directly (FWHM from approximately 15 nm to 20 nm). They have saturated color appearances and chromaticity coordinates very near the spectrum locus.

1.3. Goals and hypotheses

To our knowledge, no standards development organization (SDO) is developing specifications for SSL products with chromaticities outside of the ANSI quadrangles for outdoor general lighting applications. At the same time, SSL chip manufacturers are developing products outside of these quadrangles, especially products marketed as having CCTs lower than 2200 K and/or an "amber" color appearance. Without standardized definitions for light sources with chromaticities outside of the ANSI quadrangles, lighting professionals are left to define their own terms, often leading to confusion. Terms observed in publicly available product literature (DesignLights Consortium 2022) includes the following:

- "Amber CCT", "CCT = 2000 K", "Filtered LED", "CCT = 2K – 580 nm", "CCT = 2K – 595 nm", "CCT = AM – Amber, 595 nm",

- "Peak dominant WL 592m and 595 nm ± 2.5 nm", "PC Amber, Peak intensity 610 nm", "590 nm Amber", "AMBPC (Amber PC)", "AMBWL (wavelength limited)", "A (Amber 595 nm)", "R (Red, 620 nm)"

- "Red-Orange (1000 K)", "Narrow-band 590nm +/- 5nm for wildlife and observatory use", "HPS replacement", and "Amber (1541 K)".

- "FWC Certification, AMBER light Turtle friendly", "FWC Approved", "AM – amber LED turtle friendly 585-595nm", "Wildlife-Friendly Amber (585 – 595 nm)"

There is no uniform method to accurately interpret the meaning of these specifications. Without a consistent lexicon, lighting professionals have no framework with which to consistently compare, specify or validate lighting products with chromaticities outside of the ANSI quadrangles. To this end, we offer *Expanded* chromaticity quadrangles for target CCTs of 2000

K and 1800 K using the ANSI C78.377-2017 framework (NEMA 2017) and propose chromaticity tolerances and specification nomenclature for direct-emission (DE) and phosphor-converted (PC) LEDs that are nominally "amber", "orange", and "red". These specifications offer a parsimonious approach to specifying light sources with non-white chromaticities.

We then test the impact of these new specifications on relative sky glow with the expectation that, on average, non-white light sources with chromaticities outside of the ANSI quadrangles will have lower relative sky glow than white light sources with chromaticities in the ANSI quadrangles.

2. Methodology

To compare the performance of SPDs within and outside of the ANSI quadrangles, the following process was followed: 1. Develop chromaticity quadrangles for CCTs below 2200 K, 2. Determine a reasonable chromaticity tolerance for PC Amber LEDs, 3. Determine a method for generating DE Amber and PC Amber spectral power distributions (SPDs), 3. Simulate SPDs, 4. Compile a set of real, commercially available LED SPDs for comparison, 5. Compute relevant spectrally derived measures, and 6. Compare.

2.1. *Expanded* nominal CCT quadrangles

Chromaticity quadrangles for nominal CCTs of 2000 K and 1800 K were generated using a process inspired by ANSI C78.377-2017 (NEMA 2017). These are henceforth referred to as the "*Expanded*" quadrangles. Quadrangles with centers aligned with the *Basic* ANSI quadrangles are the "*Expanded Basic"* quadrangles; those with centers aligned with the *Extended* ANSI quadrangles are the "*Expanded Extended*" quadrangles. The *Expanded Extended* quadrangles were developed to complement the "*Expanded Basic*" quadrangles and are not based on scientific evidence that chromaticities in this region appear more "natural", "neutral", or "preferred" than chromaticities closer to the Planckian Locus.

The process for their development is described below.

1. Fit a line to the top limit of the 7-step *Basic* ANSI quadrangles, that extends from the existing quadrangles to the spectrum locus (dashed line under Point 1, **Figure 1**). The equation for that line is the following:

$$y = -2.2187x^2 + 2.3015x - 0.1621 \quad (R^2 = 1) \tag{1}$$

2. Fit a line to the spectrum locus from 580 nm to 780 nm, which is near the "amber" region (Point 2, **Figure 1**). The equation for that line is the following:

$$y = -0.996x + 0.997 \quad (R^2 = 1) \tag{2}$$

3. Find the intersection point of the lines described in Step 1 and Step 2 (Point 3, **Figure 1**).
    - The intersection point has an (x,y) chromaticity of (0.5706, 0.4288), a CCT of 1770 K, and a D_{uv} of 0.0070.
4. Fit a line to the bottom limit of the 7-step *Basic* ANSI quadrangles (dashed line under Point 4, **Figure 1**). The equation for that line is the following:

$$y = -2.4619x^2 + 2.4243x - 0.1999 \quad (R^2 = 1) \tag{3}$$

5. Find the intersection point between the line in Step 4 (bottom limit of the 7-step *Basic* ANSI quadrangles), and the line connecting the intersection point from Step 3 with the chromaticity of a blackbody radiator at 1770 K. The intersection point (Point 5, **Figure 1)** has an (x,y) chromaticity of (0.5398, 0.3914). The line formed by this point and the intersection point of Step 3 form the

rightmost boundary of the *Expanded Basic* 1800 K quadrangle. This definition of the low end of the 1800 K quadrangle was chosen to prevent monochromatic radiation from achieving a CCT designation.

6. Fit a line to the bottom limit of the 7-step *Extended* ANSI quadrangles (dashed line under Point 6, **Figure 1**). The equation for that line is the following:

$$y = -2.725x^2 + 2.5585x - 0.2372 \qquad (R^2 = 1) \tag{4}$$

7. Find the intersection between the lines from Step 5 and Step 6:
    - The intersection point has an (*x*,*y*) chromaticity of (0.5126, 0.3583) (Point 7, **Figure 1**).
8. With Steps 1 through 7 complete, the outside limits of both the 2000 K and 1800 K *Basic* and *Extended* quadrangles are defined. The next step is to determine the dividing line that will differentiate the *Basic* and *Extended* 2000 K quadrangles from the *Basic* and *Extended* 1800 K quadrangles. A process was performed to match the ANSI C78.377 nominal designations in form and intent.
    - The ANSI C78.377-2017 CCT tolerances have the form "Target CCT ± Tolerance" (NEMA 2017)). The center CCT of each quadrangle bisects the CCT range of the quadrangle. Furthermore, the tolerances approximately decrease as CCT decreases. CCT center values of 2042 K and 1859 K, with tolerances of 94 K and 89 K, were chosen for the 2000 K and 1800 K quadrangle, respectively (center CCTs shown in Figure 1). With this specification, the quadrangles are approximately equal in size with a tolerance that also decreases with CCT. With these tolerances, the dividing line between the 2000 K and the 1800 K quadrangles is at a CCT of 1948 K.
    - The intersection point between the chromaticity of the blackbody radiator with a CCT of 1948 K and the ANSI top/bottom extension lines of the *Basic* ANSI quadrangles defined in Steps 1 and 4, respectively, has an (*x*,*y*) chromaticity of (0.5193, 0.3951) (Point 8, **Figure 1**).
9. Find the intersection point between the 1948 K dividing line defined in Step 8 and the line defined in Step 6 that defines the bottom of the *Extended* quadrangles (Point 9, **Figure 1**).
10. Determine the best fit line through the centers of the *Extended* ANSI quadrangles (dashed line below Point 10, **Figure 1**). The equation for that line is the following:

$$y = -2.5889x^2 + 2.4893x - 0.2186 \qquad (R^2 = 1) \tag{5}$$

11. To find the centers of the *Extended* 2000 K and 1800 K quadrangles, Microsoft Excel Solver was used to determine the intersection point between the line defined in Step 10 and the iso-CCT lines for 2042 K and 1859 K (the target CCTs for the 2000 K and 1800 K quadrangles, respectively). See points 11a and 11b of **Figure 1**.

The *Expanded Basic* and *Expanded Extended* quadrangles and center points for nominal CCTs of 2000 K and 1800 K are shown in **Figure 2**. Specifications for the *Expanded* quadrangles are provided in **Table 1** and **Table 2**.

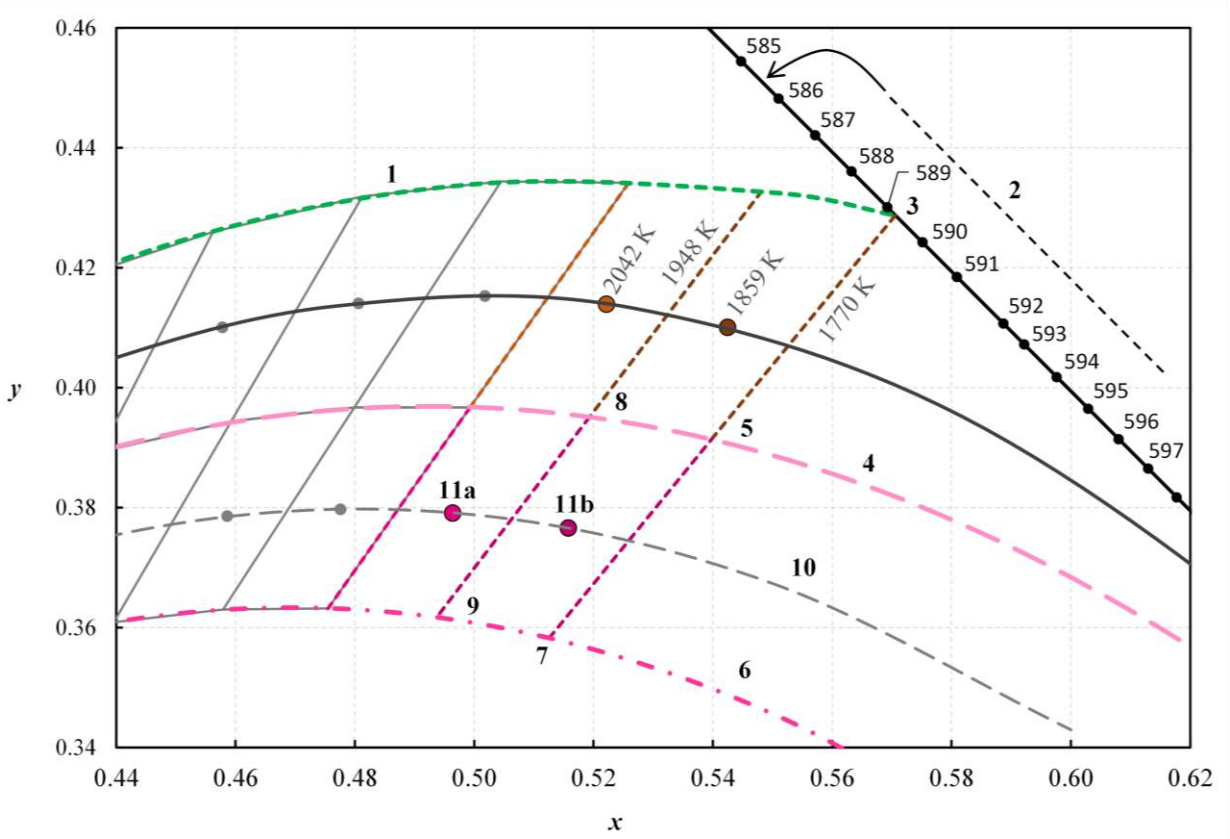

Figure 1 An enlarged portion of the CIE 1931 *xy* diagram showing the development steps of the proposed *Expanded Basic* and *Expanded Extended* quadrangles for nominal CCT designations of 2000 K and 1800 K. The numbers correspond to the development steps in the body text.

Table 1 *Expanded* nominal CCT specifications for nominal CCTs of 2000 K and 1800 K in the *Basic* (top two rows) and *Extended* (bottom two rows) specification. The "/012" nomenclature is taken from ANSI C78.377-2017 (NEMA 2017) and indicates that the *Extended* quadrangles are centered below the Planckian locus with a D_{uv} of -0.0120.

Nominal CCT Category	Target CCT and Tolerance (K)	Target D_{uv}
1800	1859 ± 89	0.0000
2000	2042 ± 94	0.0000
1800/012	1859 ± 89	-0.0120
2000/012	2042 ± 94	-0.0120

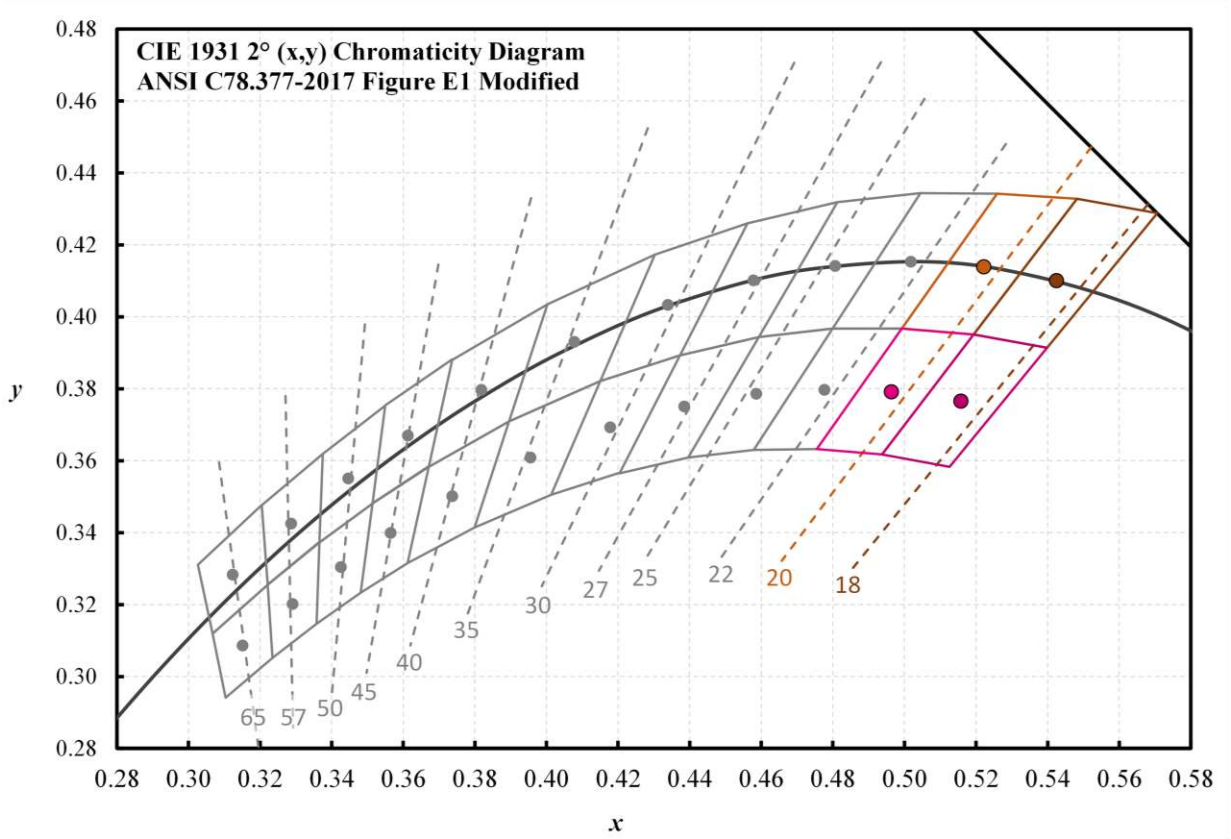

Figure 2 An enlarged portion of the CIE 1931 *xy* chromaticity diagram. Shown are the proposed *Expanded* quadrangles for CCT designations of 2000 K and 1800 K alongside the *Basic* and *Extended* ANSI C78.377-2017 quadrangles. Number labels indicate the CCT of the nearby iso-CCT line with the trailing zeros removed for clarity (e.g., "20" = "2000 K")

Table 2 Chromaticity coordinates for the center and four corners of the *Expanded* CCT quadrangles in the *Basic* (top two tows) and *Extended* (bottom two rows) specification. The "/012" nomenclature is taken from ANSI C78.377-2017 (NEMA 2017) and indicates that the *Extended* quadrangles are centered below the Planckian locus with a D_{uv} of -0.0120.

Nominal CCT Category		Center	A	B	C	D
			(x, y) tolerance quadrangle			
1800 K	x	0.5425	0.5706	0.5482	0.5193	0.5398
	y	0.4101	0.4288	0.4328	0.3951	0.3914
2000 K	x	0.5222	0.5482	0.5259	0.4993	0.5193
	y	0.4139	0.4328	0.4342	0.3967	0.3951
1800/012	x	0.5158	0.5398	0.5193	0.4937	0.5126
	y	0.3766	0.3914	0.3951	0.3617	0.3583
2000/012	x	0.4964	0.5193	0.4993	0.4755	0.4937
	y	0.3791	0.3951	0.3967	0.3632	0.3617

This is an Accepted Manuscript of an article published by Taylor & Francis in LEUKOS on 01/05/2022, available online: https://www.tandfonline.com/doi/full/10.1080/15502724.2022.2121285

2.2. Chromaticity boundary for phosphor-converted amber ("PC Amber") LEDs

Phosphor-converted amber LEDs are often binned according to their chromaticity, though the exact bin depends on manufacturer and the potential application. Three methods for defining the chromaticity limits for simulating PC Amber SPDs were considered:

1. **Specification standards from outside of the architectural lighting industry:** Examples include the "Yellow" specification of the Institute of Traffic Engineers (ITE)(Joint Industry and Traffic Engineering Council Committee 2005) or the "Yellow (Amber)" specification of SAE International (Society of Automotive Engineers 2020). These specifications have the benefit of being well-defined and referenceable. They have the drawback of likely being too restrictive for general-purpose outdoor illumination; they also guarantee that all outdoor architectural lighting products have the same or similar color appearance as traffic and transportation indicator lights, which may be undesirable.

2. **Using a measure of visual tolerance:** Conceptually, a measure of visual tolerance could define the boundary. The most familiar tolerances are MacAdam's ellipses (MacAdam 1942; MacAdam 1943; MacAdam 1985). Importantly, MacAdam's ellipses near the spectrum locus at 590 nm do not orient in the direction of the spectrum locus and the range of chromaticities for existing PC Amber LEDs is situated along the short axis (the "b" axis) of the ellipse. An impractically large MacAdam ellipse of many more than 25 steps (i.e., 25 multiples of the standard deviation of color matching, SDCM) is needed to cover this range of chromaticities and would extend past the Planckian locus. For this reason, such an approach is not pragmatic.

3. **Using tolerances of real PC Amber LED products:** the range of chromaticities that LED chip manufacturers consider PC Amber is well-defined and publicly available. These tolerances vary amongst manufacturers. One method for defining a chromaticity tolerance for PC Amber is to encapsulate—or "outline"—the tolerances from all manufacturers (**Figure 3 and Table 3**). This method has the benefit of being highly applicable to real architectural lighting products since these are the actual boundaries for real products; this method has the drawback of being based on tolerances whose development is not clearly described in publicly available literature.

For this analysis, we used the tolerance of real PC Amber LED products (Method 3) when generating PC Amber LEDs since it is most directly relevant to the practice of architectural lighting. The chromaticity boundary for this tolerance is provided in **Table 3**.

Table 3 CIE 1931 *xy* chromaticity coordinates for the boundary of real PC Amber LED products shown in Figure 3.

x	*y*
0.5400	0.4590
0.5280	0.4430
0.5478	0.4260
0.5469	0.4249
0.5700	0.4100
0.5715	0.4099
0.5730	0.4089
0.5787	0.4033
0.5926	0.4074

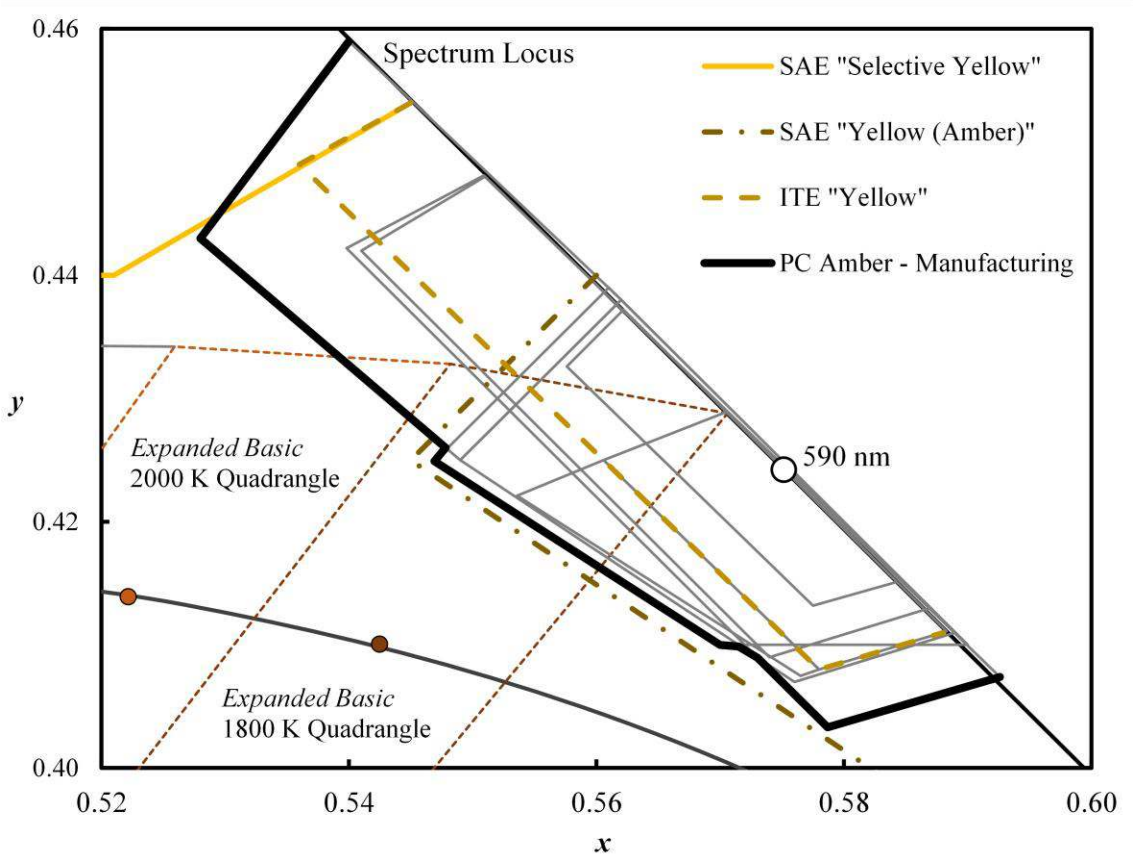

Figure 3 An enlarged portion of the CIE 1931 *xy* diagram showing PC Amber chromaticity bins from various manufacturers (thin solid grey lines), and a composite PC Amber bin determined by outlining the limits of all bins (thick black line). Shown for reference are the SAE "Selective Yellow", SAE "Yellow (Amber)", and the ITE "Yellow" chromaticity boundaries. Also shown are the *Expanded Basic* 2000 K and 1800 K quadrangles (thin dashed lines).

2.3. Simulated SPDs

A set of polychromatic SPDs was generated to compare the range of performance of SPDs in the ANSI quadrangles and those with the previously described designations of DE amber, PC amber, and the *Expanded Basic* and *Expanded Extended* CCT quadrangles.

2.4 Simulated SPDs in the CCT quadrangles

A base set of real, commercially available LED SPDs (**Figure 4**) was used to estimate the range of performance that is practically achievable with currently available LED chips/packages. SPDs were downloaded from the websites of chip manufacturers, digitized by hand from publicly available information, or provided directly from the manufacturer (anonymized personal communication). SPDs for LEDs near the extents of the visible spectrum, such as "violet" and "far red", were not used in this analysis since these are near the tails of the photopic luminous efficiency function and not common in architectural lighting for outdoor environments. "Violet" radiation is particularly detrimental to astronomical observations (anonymized personal communication) and is discouraged for outdoor nighttime use.

An all-possible-combinations approach was performed using various subsets of the 10 base LED chips. Ten thousand (10,000) composite SPDs were generated as random linear combinations of randomly selected base LEDs, combining 2, 3, 4, 5, 6, 7, 8, and 9 SPDs. This subset approach

was done to expand the coverage of chromaticity space of the generated composite SPDs. A final 10,000 composite SPDs were generated using all 10 base SPDs. A total of 90,000 composite SPDs were generated in this way (10,000 base SPDs for each of 9 combinations) then filtered for inclusion in the ANSI *Basic* and *Extended* quadrangles and the *Expanded* quadrangles for CCTs of 2000 K and 1800 K detailed in **Section 2.1. *Expanded* nominal CCT quadrangles**. A total of 12,245 composite SPDs remained after filtering for analysis. This data set represents a large range of variability that is based on realizable SPDs. It does not necessarily represent the range of theoretically possible values.

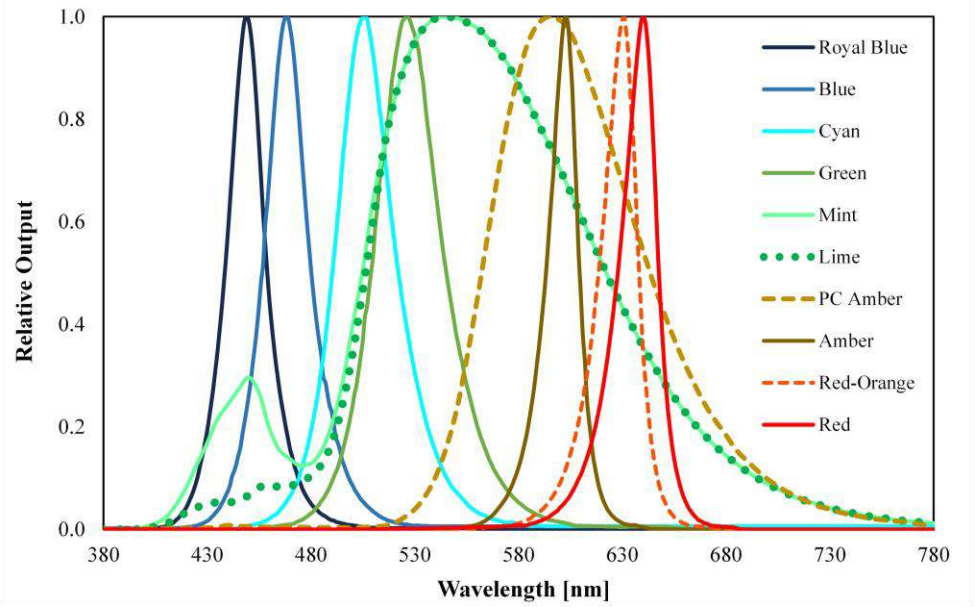

Figure 4 Relative SPDs used for polychromatic simulations based on real, commercially available LED products. Variation in line type is intended to increase readability.

2.5 Simulating PC Amber LEDs

The spectrum of a PC Amber LED is made up of two principal components: the short wavelength "hump" from the "blue pump" LED and a broadband spectral emission from a phosphor. To determine practical simulation parameters for realistic PC Amber LEDs, we collected the SPDs of commercially available PC Amber LEDs and short-wavelength LEDs and measured their peak wavelengths and spectral widths.

Measurements showed the broadband component of real PC Amber LEDs—the part of the spectrum relating to the phosphor—having peak wavelengths of 595 nm to 605 nm, and full width at half-maximum (FWHM) values ranging from 79 nm to 87 nm. The short wavelength LED chips selected (i.e., those with nominal descriptors of "violet", "blue", or "royal blue") had peak wavelengths from 425 nm to 469 nm and FWHM values from 16 nm to 36 nm. For this simulation, the range of peak and FWHM values was extended to increase variability relative to real products.

To simulate PC Amber LEDs, we generated two-component SPDs with Gaussian distributions having the following spectral parameters with chromaticities in the PC Amber boundary defined in **Table 3**:

Gaussian 1: Peak = 415 nm to 480 nm | FWHM = 12 nm to 40 nm

Gaussian 2: Peak = 500 nm to 630 nm | FWHM = 50 nm to 100 nm

Some SPDs generated in this way are shown in **Figure 5**.

2.6 Simulating DE Amber LEDs

To determine practical simulation parameters for DE Amber LEDs, we collected the SPDs of commercially available DE Amber LED chips and measured their peak wavelengths and spectral widths. These chips had peak wavelengths of 593 nm, 595 nm, and 603 nm and FWHM values of approximately 17 nm.

The range of values for simulated DE Amber SPDs was extended slightly beyond the commonly available peak and FWHM values to increase variability relative to real products. Gaussian distributions were generated with a peak wavelength varying from 585 nm to 600 nm and a FWHM ranging from 10 nm to 24 nm. Some SPDs generated in this way are shown in **Figure 5**.

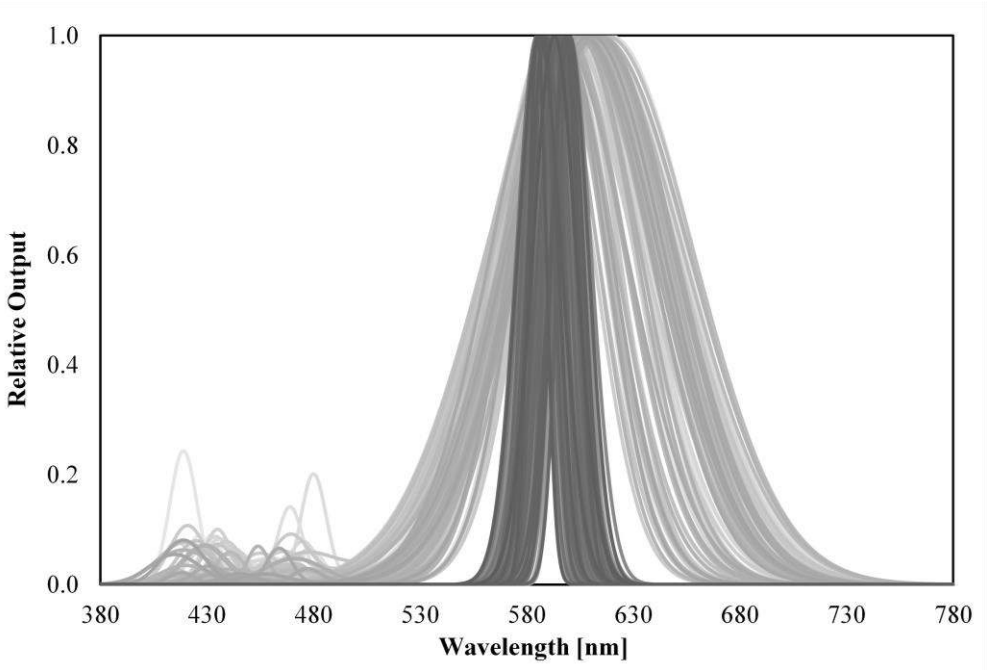

Figure 5 A sample of simulated DE Amber (dark grey) and PC Amber (light grey) SPDs.

2.7. Performance analyses with real SPDs

To compare the performance of simulated SPDs to real SPDs, we compiled a set of real SPDs taken from commercially available phosphor-converted white LEDs. These SPDs were extracted from anonymized .SPDX files that were submitted to the DesignLights Consortium (DLC) for tested LED luminaires as part of their qualification to the DLC's SSL Qualified Products List (QPL). A total of 888 SPDs were compiled. Per DLC's V5 Technical Requirements, these outdoor LED products have CCTs per ANSI C78.337-2017 ranging from 2200K to 6500K. All the luminaires had (x, y) chromaticities falling in the ANSI *Basic* Quadrangles.

In addition, SPDs for commercially available DE Amber and PC Amber LEDs were downloaded from the websites of chip manufacturers, digitized by hand from publicly available information, or provided directly from the manufacturer (anonymized personal communication). Recently developed PC LED light sources with CCTs near 2000 K and 1800 K were provided directly by the manufacturer (anonymized personal communication).

This is an Accepted Manuscript of an article published by Taylor & Francis in LEUKOS on 01/05/2022, available online: https://www.tandfonline.com/doi/full/10.1080/15502724.2022.2121285

2.8. Relevant spectrally derived measures

Relevant spectrally derived measures were computed for all simulated SPDs. We evaluated spectrally derived measures related to general lighting quality and those potentially useful for reducing the negative impacts of ALAN. The selected measures are briefly described below, and their formulae and thresholds are shown in **Table 4**:

Percent radiation below 500 nm (P_{500}): The proportion of an SPD's radiation between 400 nm and 500 nm is a spectrally derived measure used in the County Code of the Big Island of Hawaii to qualify products that may be installed on the island. Less than 2% of an SPD's radiation in this spectral band is permitted. The Big Island of Hawaii is notable for having low levels of light pollution (County of Hawaii 1983).

Similarly, the proportion of an SPD's radiation between 380 nm and 499 nm is used by the Ministry for the Environment of the Republic of Chile. No more than 15% of an SPD's radiation is permitted in this band for astronomically protected areas (Republic of Chile 2013). New draft legislation from the Republic of Chile sets a limit of 1% in this spectral band for astronomically sensitive areas and 15% for the rest of the territory in the republic (Republic of Chile 2021). Note that the spectral range for the denominator is 380 nm to 780 nm, compared to a spectral range of 400 nm to 700 nm for that used in the County Code of the Big Island of Hawaii.

Because the two measures are nearly identical for our dataset (R^2 = 0.9995)—i.e., our SPDs contain no radiation between 380 nm and 400 nm (the lower limit) and 499 nm is one nanometer lower than 500 nm (the upper limit)—we will report only the computed values using the definition of the County Code of the Big Island of Hawaii (**Table 4**).

For reference, the wavelength of 500 nm approximately bisects the scotopic sensitivity curve (actual bisection point is near 503 nm) and is near the curve's peak sensitivity at 505 nm.

Percent radiation below 520 nm (P_{520}): The proportion of an SPD's radiation below 520 nm is a spectrally derived measure used by the International Dark Sky Association (IDA) to qualify products for their "Innovation" seal of approval, which is designed to "encourage a best-in-class lighting development that significantly reduces light pollution and nocturnal habitat disruption" (International Dark-Sky Association (IDA) 2021). No more than 7% of an SPD's radiation is permitted below 520 nm.

Percent radiation below 530 nm (P_{530}): The proportion of an SPD's radiation below 530 nm is a spectrally derived measure used by the Community Friendly Lighting (CFL) program of the Smart Outdoor Lighting Alliance (SOLA) to qualify luminaires. To achieve the SOLA CLP Certificate, no more than 25% of an SPD's radiation is permitted between 430 and 530 nm (Smart Outdoor Lighting Alliance (SOLA) 2017).

The P_{530} measure used by SOLA uses a wavelength range of 430 nm to 530 nm in the numerator, rather than the lower bound of 400 nm that we used (**Table 4).** The two measures are highly correlated (R^2 = 0.9992) for our dataset. We report only the values using the lower bound of 400 nm for consistency and comparison with other response measures.

Percent radiation below 560 nm (P_{560}): The proportion of an SPD's radiation below 560 nm is a spectrally derived measure used by the Florida Fish and Wildlife Conservation Commission (FWC) to certify luminaires for their "Wildlife Lighting Certification Program" (Florida Fish And Wildlife Conservation Commission). The program permits no radiation (0%) below 560 nm. The Wildlife Lighting certification is intended to reduce the negative impact of ALAN on sea turtle nesting sites on Florida beaches.

Scotopic-to-Photopic Ratio (S/P): The Scotopic-to-Photopic ratio describes the ratio of a light source's radiation that is coincident with the Scotopic Luminous Efficiency function, V'(λ), to its radiation coincident with the Photopic Luminous Efficiency Function, V(λ). Scotopically weighted irradiance appears in the literature in multiple forms (Aubé et al. 2013; Luginbuhl et al. 2014; Zukauskas et al. 2014; Kinzey et al. 2017; Galadí-Enríquez 2018; Bará et al. 2020). An S/P ratio less than 1.2 was used in a previous version of the IDA Fixture Seal of Approval program (International Dark-Sky Association (IDA) 2015), but is no longer.

"Azul"-to-Photopic Ratio (A/P): The Azul-to-photopic ratio describes the ratio of a light source's radiation between 380 nm and 500 nm to its radiation coincident with the Photopic Luminous Efficiency Function, V(λ). Azul is the Spanish word for blue. The A/P Ratio is used by The Technical Office for the Protection of Sky Quality (TOPC) of the Institute of Astrophysics of the Canary Islands (IAC) to define "warm white" and "super warm white" LEDs with thresholds of 0.25 and 0.15, respectively (Institute of Astrophysics of the Canary Islands (IAC) 2022). It is also included in the draft regulation of Andalusia in southern continental Spain (Government of Andalusia 2019) and in the Revision of the EU Green Public Procurement Criteria for Road Lighting (Donatello et al. 2018) in the logarithmic scale of Galadi-Enriquez (2018), in the form of the G Spectral index [$G = -2.5*\log_{10}(A/P)$], but with the same effective limits as IAC. For simplicity, we will report only the A/P values.

Relative Sky Glow (RSG): RSG was computed using the Excel Sky Glow Comparison Tool (Pacific Northwest National Laboratory (PNNL)) accompanying the work of Kinzey et al. (2017) that we adapted to perform batch calculations. Parameters that may be varied include observer location, atmospheric condition, viewer adaptation state, percent uplight (%UL), and relative lumen output (RLO). Because RSG is a relative calculation, specification of the "baseline" condition (henceforth referred to as the "reference" condition) is necessary.

All computations used a high-pressure sodium (HPS) reference source for direct comparison to Kinzey et al. (2017) as well as the historical importance of HPS in streetlighting. To isolate the impact of light source SPD, %UL was set to 0% for both the test and reference conditions, and the RLO of the test source was set equal to the lumen output of the HPS reference source (i.e., RLO = 1.00 = 100%). The viewer adaptation state was set to "Scotopic". Scotopic RSG was computed using various combinations of observer location and atmospheric condition. While the magnitude of the estimated RSG varied, the RSGs were highly correlated across combinations of parameters ($R^2 > 0.97$ for several comparisons). For simplicity, we present only the results using an observer location of "Near" and atmospheric conditions of "Clear, Low Particulate". The value of RSG using these computational parameters will henceforth be referred to as "RSG" for brevity.

Measures of color rendition from ANSI/IES TM-30-20 (IES 2019) were also computed. Legacy measures of color rendition such as R_a and R_9 from CIE 13.3-1995 (CIE 1995) were also computed for historical reference. We note here that standardized measures of color rendition have questionable utility in the context of outdoor nighttime lighting where mesopic adaptation is likely and light source chromaticity may not permit full chromatic adaptation. We nonetheless use these measures for lack of standardized calculations under mesopic conditions and/or for light sources that may not be perceptibly white.

Table 4 Formulae, thresholds, and references for spectrally derived measures

Symbol	Formula	Threshold	Source
P_{500}	$P_{500} = \frac{\sum_{400}^{\mathbf{500}} SPD(\lambda)}{\sum_{400}^{700} SPD(\lambda)}$	< 0.02 (2%) ≤ 0.15 (15%)[a,c] ≤ 0.01 (1%)[b,c]	County Code of the Big Island of Hawaii (County of Hawaii 1983) Republic of Chile (Republic of Chile 2013; Republic of Chile 2021)
P_{520}	$P_{520} = \frac{\sum_{400}^{\mathbf{520}} SPD(\lambda)}{\sum_{400}^{700} SPD(\lambda)}$	≤ 0.07 (7%)	The "Innovation" seal of the International Dark Sky Association (International Dark-Sky Association (IDA) 2021)
P_{530}	$P_{530} = \frac{\sum_{400}^{\mathbf{530}} SPD(\lambda)}{\sum_{400}^{700} SPD(\lambda)}$	≤ 0.25 (25%)	The Community Friendly Lighting Program of the Smart Outdoor Lighting Alliance (Smart Outdoor Lighting Alliance (SOLA) 2017)
P_{560}	$P_{560} = \frac{\sum_{400}^{\mathbf{560}} SPD(\lambda)}{\sum_{400}^{700} SPD(\lambda)}$	$= 0.0$ (0%)	The "Wildlife Lighting" seal of the Florida Fish and Wildlife Conservation Commission (Florida Fish And Wildlife Conservation Commission)
S/P	$\mathrm{S/P} = \frac{1700 \sum_{380}^{780} SPD(\lambda)\, V'(\lambda)}{683 \sum_{380}^{780} SPD(\lambda)\, V(\lambda)}$	--	(Berman 1992)
A/P	$\mathrm{A/P} = \frac{\sum_{380}^{500} SPD(\lambda)}{\sum_{380}^{780} SPD(\lambda)\, V(\lambda)}$	≤ 0.25 (25%)[d] ≤ 0.15 (15%)[e]	(Donatello et al. 2018; Government of Andalusia 2019; Institute of Astrophysics of the Canary Islands (IAC) 2022)

[a] Existing threshold for astronomically sensitive areas in the Republic of Chile (Republic of Chile 2013). In proposed legislation (Republic of Chile 2021), this threshold is used for all areas of the republic that are not astronomically sensitive

[b] In proposed legislation of the Republic of Chile (Republic of Chile 2021), this threshold will be used for astronomically protected areas.

[C] Note the spectral ranges used by the Republic of Chile to compute P_{500} vary slightly from those used by the County Code of the Big Island of Hawaii. Because the two definitions are highly correlated for our dataset (R^2 = 0.9995), all thresholds are evaluated using P_{500} from the County Code of the Big Island of Hawaii for simplicity.

[d] Threshold for "Warm White" LEDs per IAC (Institute of Astrophysics of the Canary Islands (IAC) 2022)

[e] Threshold for "Super Warm White" LEDs per IAC (Institute of Astrophysics of the Canary Islands (IAC) 2022)

3. Results

Figure 6 show boxplots of P_{500} (top left), P_{520} (top right), P_{530} (bottom left), and P_{560} (bottom right)—i.e., measures of the percent radiation between 400 nm and the specified upper wavelength—as a function of categorical chromaticity for the simulated SPDs with CCTs below 3500 K. On average, SPDs with lower CCTs have lower percent radiation below all thresholds. Importantly, however, there is substantial overlap across CCTs such that a single threshold passes through the range of multiples CCTs (including the PC Amber and DE Amber designations).

Notable observations from **Figure 6** include the following:

- Most, but not all, simulated DE Amber LEDs comply with the FWC "Wildlife Lighting" certification. No other simulated SPD complies, including PC Amber. This is consistent with the FWC certification restriction on the use of PC Amber LEDs.
- Most simulated SPDs at a CCT of 3000 K or lower comply with SOLA CFL. This is consistent with a statement made by SOLA (Smart Outdoor Lighting Alliance (SOLA) 2017): "light sources with CCT of 3000 K or less will typically have <25% SPD below 530nm."
- A very small proportion of simulated SPDs at 2200 K comply with the IDA "Innovation" seal of approval. No other SPDs within the ANSI quadrangles comply. Many more simulated SPDs within the 1800 K and 2000 K *Expanded* quadrangles comply. Most simulated PC Amber and all simulated DE Amber SPDs comply.
- No simulated SPDs within the *Basic* or *Expanded* ANSI quadrangles comply with Hawaii's county code, which is consistent with the lighting strategy on the island of filtering PC White LEDs (anonymized personal communication). A handful of simulated SPDs within the *Expanded* quadrangles comply. Many simulated PC Amber and all simulated DE Amber SPDs comply.
- Most SPDs with a CCT at 2700 K or below comply with the current legislation in the Republic of Chile for astronomically protected areas (i.e., $P_{500} \leq 15\%$); Only DE Amber and some PC Amber SPDs comply with draft legislation that resets the threshold to one percent (i.e., $P_{500} \leq 1\%$).

Overall, the FWC "Wildlife Lighting Certification program" is the strictest specification; second is the draft limit for astronomically protected areas in the Republic of Chile; third is the County code of the Big Island of Hawaii; fourth is the "Innovation" seal of approval from IDA; and least strict are the limits for SOLA CFL and the existing legislation in the Republic of Chile, both of which perform similarly.

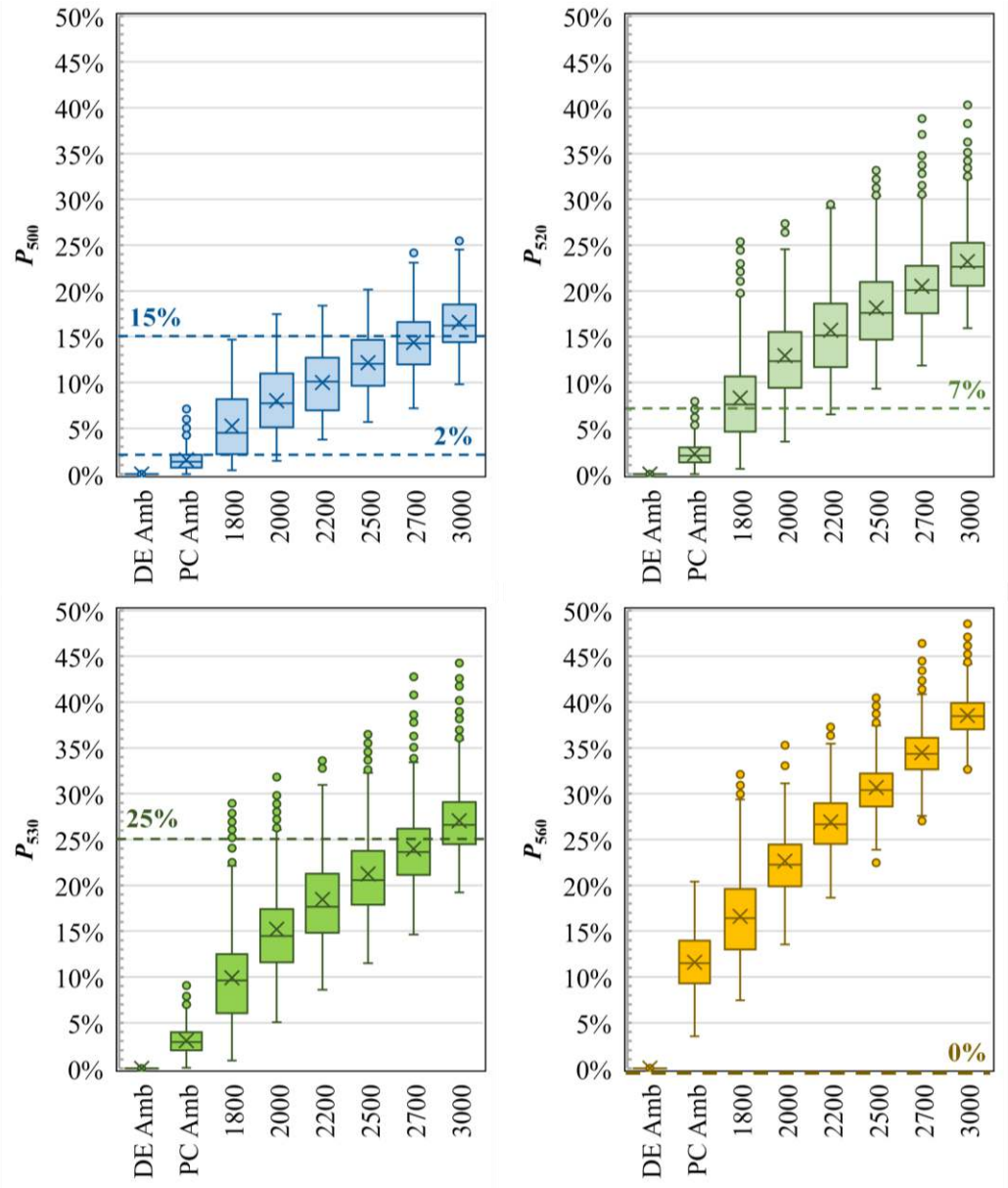

Figure 6 (Top left) P_{500} as a function of categorical chromaticity for simulated SPDs with CCTs below 3500 K. Categorical CCT—from left to right—includes direct-emission amber, phosphor-converted amber, the *Expanded* 1800 K and 2000 K CCT quadrangles, and the ANSI CCT quadrangles up to 3000 K. The horizontal dashed line at 2% shows the maximum threshold for the Hawaii County Code; the horizontal dashed line at 15% shows the threshold for astronomically protected areas in the Republic of Chile. Draft legislation from the Republic of Chile sets the threshold for astronomically protected areas to 1% (not shown to maintain clarity) and 15% for everywhere else in the republic. No simulated SPD within an ANSI CCT quadrangle complies with the Hawaii County Code (P_{500} < 2%) nor the draft limits for astronomically protected areas in the Republic of Chile. (Top right) P_{520} as a function of categorical chromaticity. The horizontal dashed line shows the maximum threshold for the IDA "Innovation" Seal of Approval. Very few SPDs in the ANSI quadrangles comply with the IDA "Innovation" Seal of Approval ($P_{520} \leq 7\%$). (Bottom left) P_{530} as a function of categorical chromaticity. The horizontal dashed line shows the maximum threshold for SOLA CFL. Some SPDs at 3000 K and most SPDs at 2700 K or below comply with the SOLA CFL ($P_{530} \leq 25\%$). (Bottom right) Percent radiation below 560 nm as a function of categorical chromaticity. The horizontal dashed line shows the threshold for FWC. No SPDs other than DE Amber comply with the FWC threshold ($P_{560} = 0\%$).

Boxplot description: The "x" represents the average; the middle horizontal bar is the median. The ends of the box represent the first and third quartiles (the difference of which is the Interquartile Range, IQR). The circle data points represent outliers. When there are no outliers, the "whiskers" represent the maximum and minimum of the data. When there are outliers—defined as a point that is greater than 1.5*IQR—the whiskers represent the local maximum and minimum, which are the values of the largest and smallest values that are not outliers.

This is an Accepted Manuscript of an article published by Taylor & Francis in LEUKOS on 01/05/2022, available online: https://www.tandfonline.com/doi/full/10.1080/15502724.2022.2121285

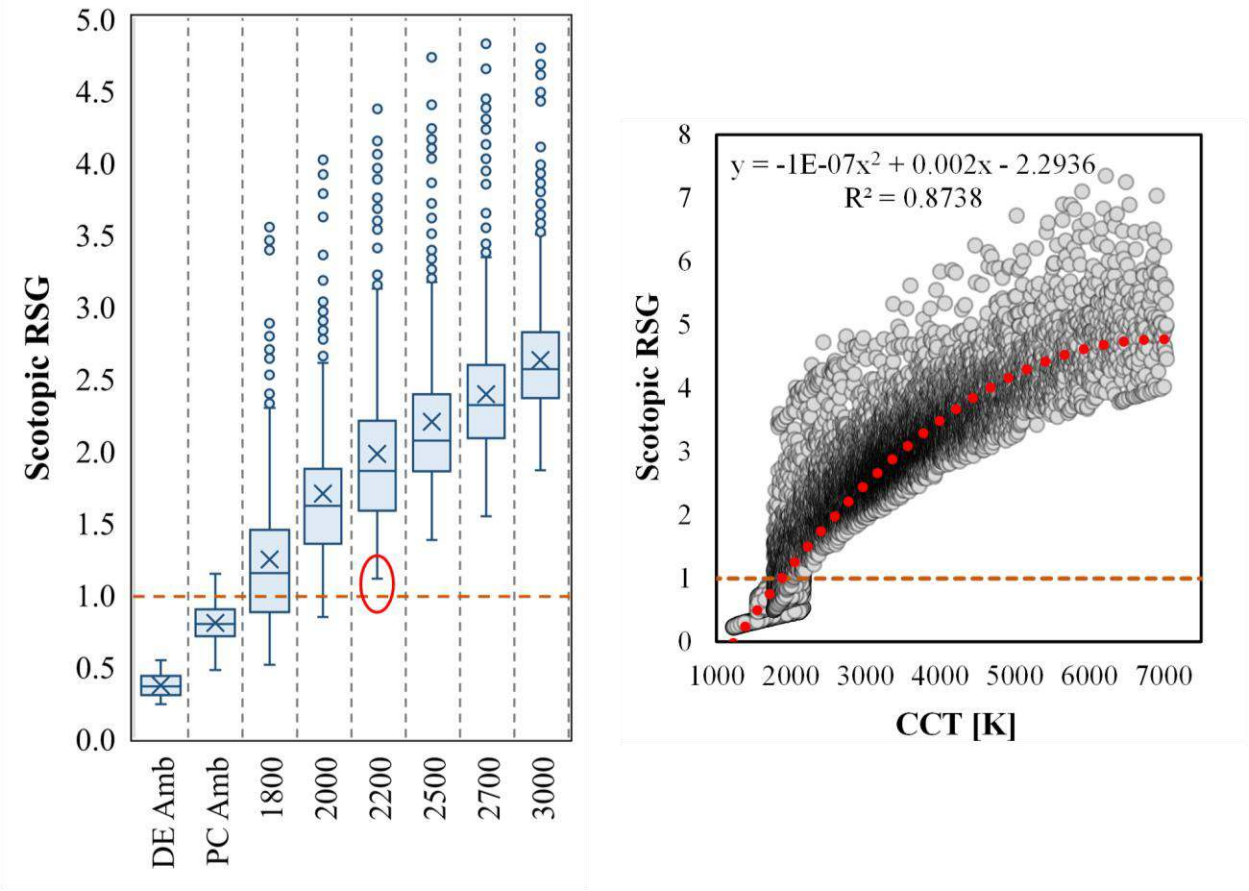

Figure 7 Scotopic RSG as a function of categorical chromaticity (left) and continuous CCT (right). The horizontal dashed orange line represents the RSG of the high-pressure sodium (HPS) reference condition. On average, RSG decreases as CCT decreases but there is substantial overlap especially between adjacent nominal CCTs. Most simulated PC Amber SPDs and all DE Amber SPDs have lower RSG than HPS. The red circle indicates that no simulated SPD within an existing ANSI C78.377 quadrangle has a lower RSG than HPS. CCT is among the worst predictors of Scotopic RSG.

Figure 8 shows the performance of the S/P Ratio and A/P ratio. Both S/P and A/P decrease, on average, as CCT decreases, though like other response measures there is overlap across CCTs. DE Amber and PC Amber have notably lower average S/P and A/P than SPDs with chromaticities in the CCT quadrangles. The maximum S/P ratio for a light source with an RSG less than or equal to 1.0 (i.e., better than or equal to HPS, all else being equal) is 0.684. Low variability in RSG is observed at a fixed value of S/P Ratio. The S/P Ratio is the strongest predictor of RSG of those considered; the A/P ratio is the fourth best, after P_{530} and P_{520} (**Table 5**).

LED SPDs with CCTs up to 3500 K may qualify as "warm white" (A/P ≤ 0.25), though among our simulations there were very few qualifying SPDs with CCTs of 3000 K and 3500 K. Most SPDs with chromaticities in the *Expanded* quadrangles qualify as "warm white". Very few SPDs within the ANSI quadrangles qualified as "super warm white"—those that qualify have CCTs of 2200 K and 2500 K. All DE Amber and all PC Amber SPDs are below both thresholds.

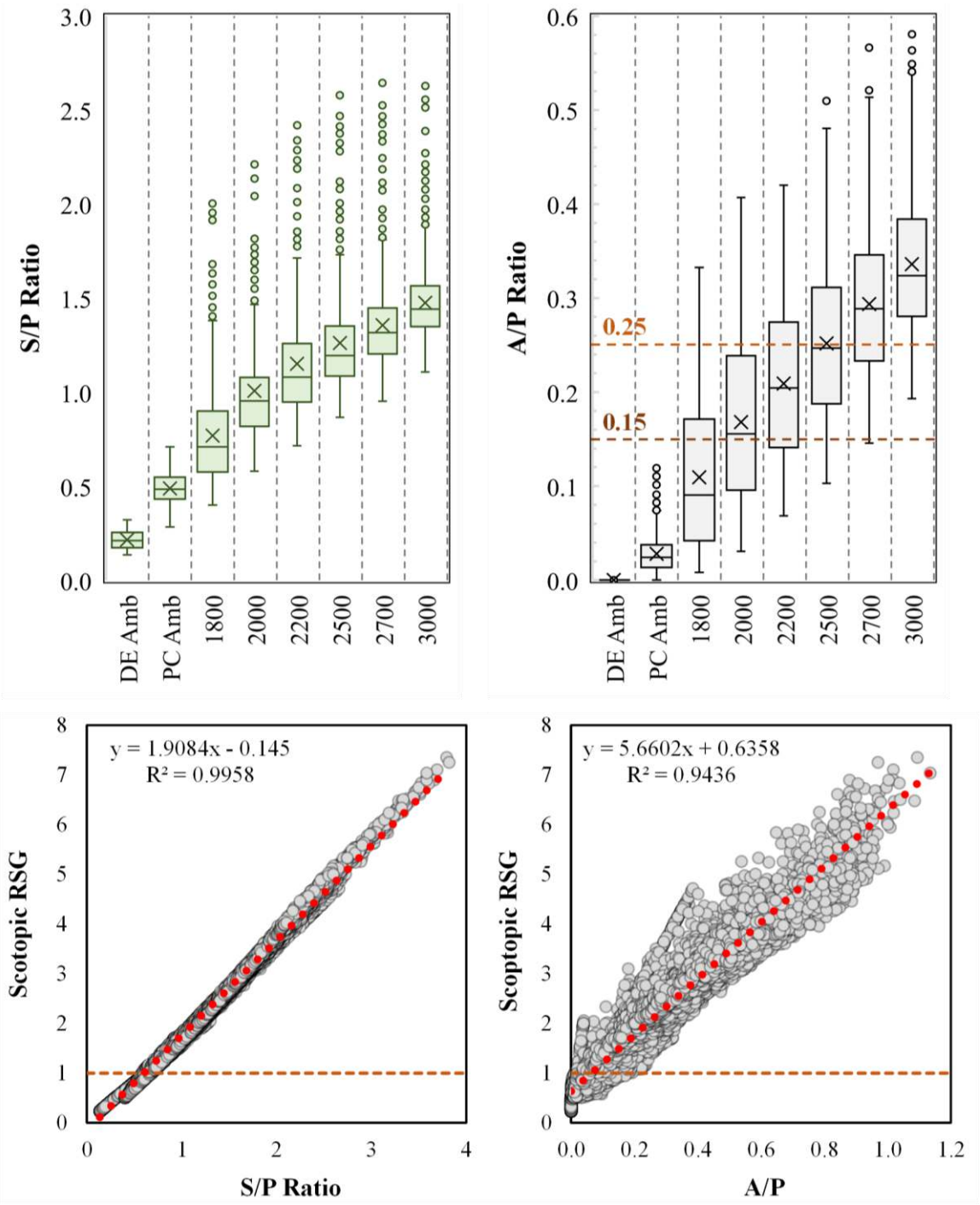

Figure 8 In the top row, the S/P Ratio (top left) and the A/P Ratio (top right) as a function of categorical chromaticity. On average, as CCT decreases, both the S/P Ratio and the A/P Ratio decrease, though there is notable overlap across adjacent CCTs. DE Amber and PC Amber SPDs have a notably lower average S/P and A/P and smaller IQR's than the SPDs in the CCT quadrangles. The horizontal dashed lines (top right) represent the thresholds for "warm white" (A/P ≤ 0.25) and "super warm white" (A/P ≤ 0.15) LEDs from the regulations of the Institute of Astrophysics of the Canary Islands (IAC) and the draft regulation of the Government of Andalusia. In the bottom row, the Scotopic RSG as a function of S/P Ratio (bottom left) and the A/P Ratio (bottom right). The horizontal, dashed orange line represents an RSG of 1.0 which is the RSG for the HPS reference condition. The red dotted line is a regression line. Both ratios and RSG are highly correlated. The S/P Ratio is the strongest predictor of RSG of those considered; the A/P ratio is the fourth best.

Figure 9 shows scatterplots of RSG as a function of P_{500}, P_{520}, P_{530}, and P_{560}. P_{520} and P_{530} are nearly equivalent predictors of RSG and are both stronger predictors than the nearly equivalent predictors P_{500} and P_{560}. All four measures are better predictors of RSG than CCT, and worse predictors than S/P Ratio (**Table 5**). Despite high coefficients of determination for all predictors, there are large differences in RSG at any fixed predictor value. For example, despite a coefficient of determination of 0.9233 for P_{500}, RSG varies from approximately 2 (two times worse than HPS) to 6 (six times worse than HPS) at a P_{500} of approximately 20%.

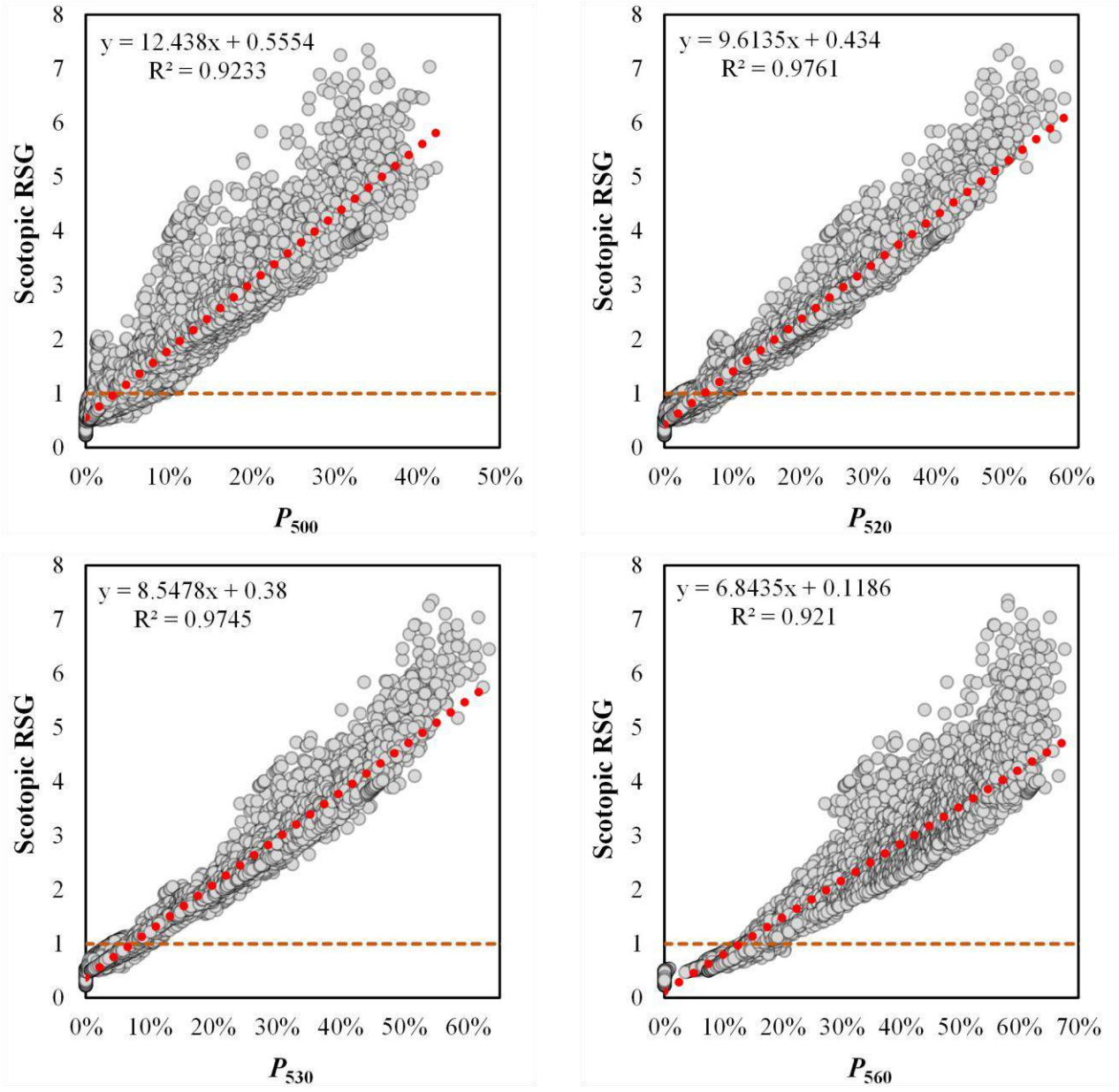

Figure 9 RSG as a function of percent radiation below 500 nm (P_{500}, top left), 520 nm (P_{520}, top right), 530 nm (P_{530}, bottom left), and 560 nm (P_{560}, bottom right). The horizontal, dashed orange line represents an RSG of 1.0 which is the RSG for the HPS reference condition. All response measures are stronger predictors of RSG than CCT and worse predictors than S/P Ratio (see Table 5). The red dotted lines are regression lines—the equations of the line and the coefficients of determination (R^2) are shown.

Table 5 Performance of various predictors of relative sky glow (RSG). R^2 is the coefficient of determination—higher is better. S is the standard deviation of the residuals—lower is better. The predictors are ordered as they appear in Section 2.8 with CCT added to the top. The S/P ratio is shown in bold as it is the best predictor for the simulated and real data.

	R^2		S	
Predictor	**Linear**	**Quadratic**	**Linear**	**Quadratic**
CCT	0.834	0.874	0.524	0.457
P_{500}	0.923	0.924	0.357	0.355
P_{520}	0.976	0.978	0.199	0.191
P_{530}	0.975	0.980	0.205	0.184
P_{560}	0.921	0.937	0.362	0.324
S/P	**0.996**	**0.998**	**0.084**	**0.063**
A/P	0.944	0.950	0.306	0.289
IES R_f	0.522	0.538	0.891	0.875
CIE R_a	0.473	0.498	0.935	0.912

On average, color fidelity decreases as CCT decreases as measured by both IES R_f and CIE R_a (**Figure 10**) On average, simulated PC Amber LEDs have lower color fidelity than those with chromaticities closer to the Planckian radiator (e.g., 3000 K), but reasonably high color fidelity is still achievable (e.g., maximum IES R_f = 72). Simulated DE Amber SPDs have nearly zero color rendering ability. IES R_f is a stronger predictor of RSG than CIE R_a (**Figure 11**), though both are notably poor predictors. Of all the predictors of RSG that were considered, CIE R_a is the worst predictor and IES R_f the second worst (**Table 5**). Most SPDs at 4000 K or below desaturate red hues and all PC Amber and Amber SPDs desaturate red hues (i.e., ANSI/IES TM-30-20 $R_{cs,h1}$ < 0%).

Trends for the real PC white, PC Amber and DE Amber SPD set are similar to those shown in **Figure 6**, **Figure 7**, **Figure 8**, and **Figure 9,** though the data is more sparse because there are fewer data points. Like the simulated dataset, no real PC white SPDs within the ANSI quadrangles have a lower RSG than HPS. All predictions of RSG are stronger with the real SPD dataset since the real products exhibit less spectral diversity than that present with our simulated SPD set. Still, the S/P Ratio was the strongest predictor of RSG (R^2 = 0.9994, S = 0.017), and color fidelity (either IES TM-30 R_f or CIE R_a) was the worst with no predictive power. CCT (R^2 = 0.9585, S = 0.140) was nearly equivalent with P_{560} (R^2 = 0.9538, S = 0.148), and lower than P_{500} (R^2 = 0.9731, S = 0.113), P_{520} (R^2 = 0.9820, S = 0.092), and P_{530} (R^2 = 0.9788, S = 0.100). All real SPDs desaturate red hues (i.e., IES TM-30 $R_{cs,h1}$ < 0%) with nearly all having more red desaturation than -10% (i.e., $R_{cs,h1}$ < -10%). All real DE Amber and PC Amber SPDs have lower RSG than HPS.

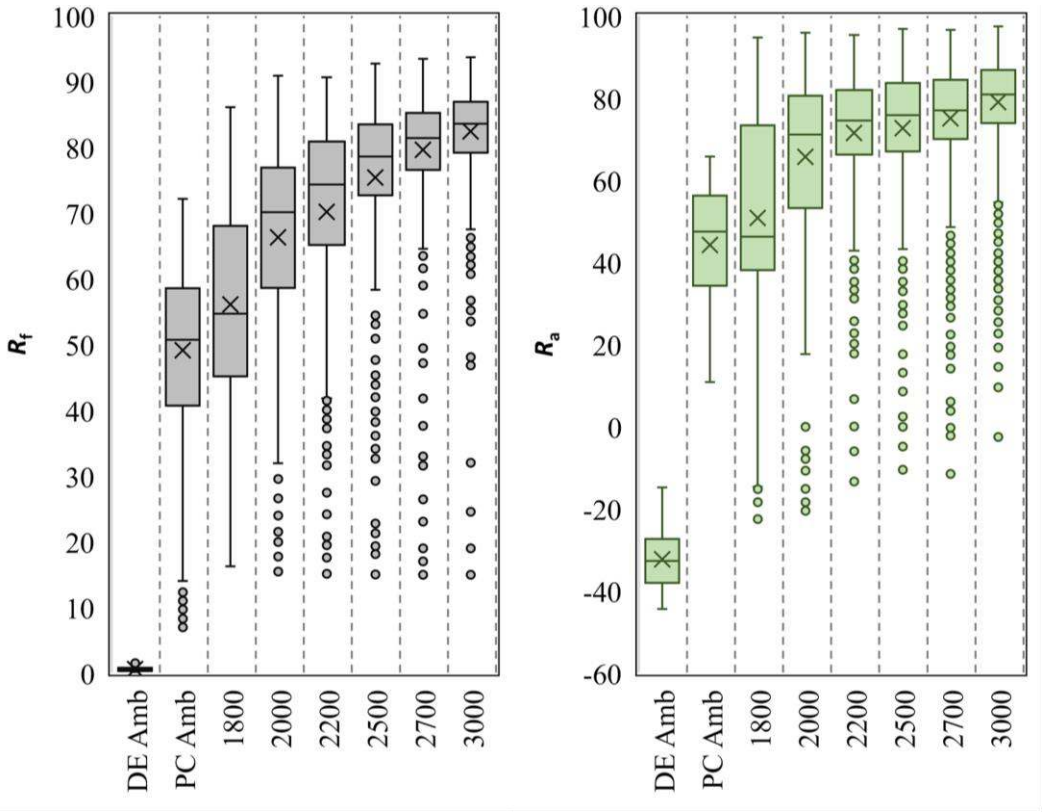

Figure 10 Boxplots of calculated color fidelity as a function of categorical chromaticity for simulated SPDs with CCTs below 3500 K. (Left) IES TM-30-20 R_f. (Right) CIE 13.3-1995 R_a. On Average, as CCT decreases, so too does average color fidelity, though there is notable overlap. DE Amber SPDs have nearly zero color rendering ability.

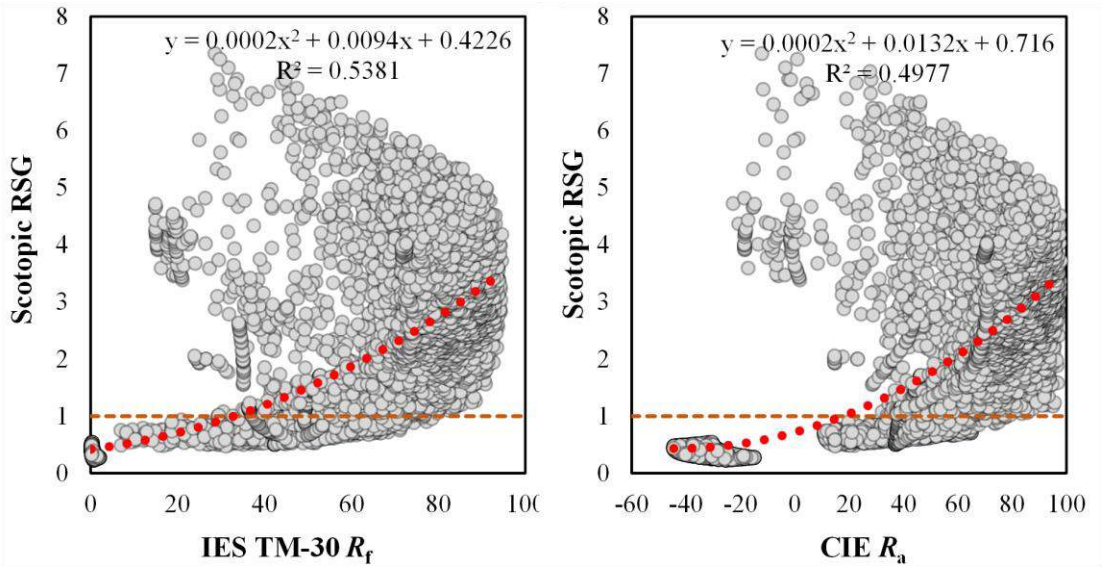

Figure 11 RSG as a function of IES TM-30 R_f (left) and CIE R_a (right). The horizontal, dashed orange line represents an RSG of 1.0, the RSG for the HPS reference condition. Color fidelity is a poor predictor of RSG; CIE R_a is the worst predictor of RSG of those considered; IES TM-30-20 R_f is the second worst. The red dotted line is a regression line—the equation of the line and the coefficient of determination (R^2) is shown.

4. Discussion

There exist many regulations, recommendations, and design guidelines for the purpose of reducing the negative ecological impacts of light at night. *Some* of those include a quantitative restriction on the short wavelength composition of the spectral power distribution—a few of which have been evaluated in this work. Many more do not provide quantitative thresholds, instead using vague descriptions such as "Limit the amount of short-wavelength light" (Hartley and Liebel 2020) (DesignLights Consortium 2022), which does not easily translate into defensible lighting specifications. Many programs and recommendations that provide quantitative limits on the SPD mostly do so by specifying maximum correlated color temperature (CCT) thresholds.

Importantly, however, **Figure 6** demonstrates that CCT cannot be used as a proxy for spectral composition of a light source's SPD, especially when limited to chromaticities within the ANSI quadrangles. **Figure 7** demonstrates that there exists sufficiently large variation in relative sky glow at any fixed categorical CCT such that CCT alone cannot be used to estimate the impact of light source SPD on relative sky glow. Furthermore, **Figure 7 (left)** demonstrates that no SPD from our dataset with a chromaticity within an ANSI quadrangle has a lower relative sky glow than high pressure sodium.

The results of the current study suggest that programs limiting the spectral content of a light source's SPD using only specifications from ANSI C78.377 will not reduce relative sky glow relative to incumbent high pressure sodium light sources. Expanding the range of standardized chromaticities has the potential to allow light sources with lower relative sky glow.

SPDs in the proposed *Expanded* chromaticity quadrangles for CCTs at 2000 K and 1800 K have lower relative sky glow, on average, than SPDs with chromaticities within the ANSI quadrangles. Some of those SPDs with a CCT of 2000 K have lower relative sky glow than HPS; many more SPDs with a CCT of 1800 K have lower relative sky glow than HPS. Most simulated PC Amber SPDs and all real PC Amber SPDs have lower relative sky glow than HPS. All DE amber SPDs, real or simulated, have substantially lower relative sky glow than HPS.

The *Expanded* CCT quadrangles for 2000 K and 1800 K are parsimoniously defined, being based on the methodology of ANSI C78.377-2017. The boundary of the PC Amber chromaticity bin is less parsimonious as it is based on tolerances published by independent LED chip manufacturers. Modifying the boundaries of the bin are unlikely to change the broad conclusion that PC Amber LEDs have more spectral impact on relative sky glow than DE Amber LEDs and less than HPS. Modifying the boundary of the PC Amber bin may, however, differentially impact some LED chip manufacturers if a change excludes any existing commercially available products.

Determining a suitable chromaticity bin for DE Amber LEDs is difficult because they are known to experience dramatic shifts in light output, peak wavelength, and chromaticity as a result of changes in operating temperature (anonymized personal communication) (Mueller-Mach et al. 2009) (DesignLights Consortium 2022). This makes a chromaticity boundary potentially unusable for specifying DE Amber LEDs with precision. Instead, DE AlInGaP LEDs (e.g., amber, orange, orange-red, and red) can be sufficiently defined by their peak wavelength since they have very high purity (i.e., their chromaticity is very near the spectrum locus).

Taken together, the designations of 2000 K, 1800 K, PC Amber, and DE Amber provide a useful stepladder to reduce, on average, the portion of estimated anthropogenic sky glow related to light source spectral power distribution. Specification basis and terminology for these designations is provided in **Table 6**, which can be used to specify non-white light sources in the outdoor nighttime environment with precision. A Microsoft Excel calculator provided as supplemental material to this manuscript can be used to help determine specifications according to **Table 6**.

The S/P ratio is a remarkably strong predictor (R^2-linear = 0.996, S-linear = 0.084) of relative sky glow (**Figure 8, bottom left**) and is the strongest of all measures considered (**Table 5**). Indeed, a good degree of correlation among scotopic RSG and S/P may be expected since both parameters are similarly constructed. In the computation of RSG, the test and reference SPDs are normalized to the same lumen output, meaning that the photopic luminous efficiency function used in the denominator in the S/P Ratio (**Table 4**) is weighted the same in both the test and reference spectra. The unweighted sky glow values are then weighted by the scotopic luminous efficiency function, the same as the numerator of the S/P Ratio. The observation that scotopic RSG and S/P Ratio are strongly correlated indicates that we may recover the relative spectral contribution to sky glow using a spectrally derived measure that is simpler to compute than RSG.

Overall, these data suggest that regulators and other program managers wishing to reduce the proportion of relative sky glow related to light source spectral power distribution may best do so by limiting the S/P Ratio of light source SPDs. Measures like CCT, CIE R_a, and IES R_f should not be used for this purpose. Measure of spectral content below cutoff wavelengths (i.e., P_{500}, P_{520}, P_{530}, P_{560}, etc.) may be useful, but have no direct spectral sensitivity link to human vision and therefore have less predictive power than the S/P Ratio. The A/P Ratio, which includes a similar photopic scaling as the S/P Ratio and RSG but no scotopic weighting, performs well, but worse than the S/P Ratio, P_{530}, and P_{520}.

The usefulness of the S/P Ratio in reducing relative sky glow is not directly transferable to other negative ecological impacts in the nighttime environment—such as species-specific effects—since such impacts were not evaluated. It is, however, firmly established that the desynchronization of the human circadian rhythm by light at night from indoor sources are more strongly mediated by short wavelength radiation (Bailes and Lucas 2013; Brown et al. 2022; Cao et al. 2023)—importantly, light sources with lower S/P Ratio contain proportionally less short wavelength radiation. Any move in the direction of reduced blue light content, and reduced ALAN from outdoor sources overall, is expected to minimize negative ecological consequences (Sanders et al. 2021).

We encourage lighting standards development organizations such as The Illuminating Engineering Society (IES), the International Commission on Illumination (CIE), The American National Standards Institute (ANSI), or others to develop quantitative, evidence-based specification structures for non-white light sources in the outdoor nighttime environment—such as that provided in **Table 6**—intended to minimize the negative impacts of anthropogenic light at night on sky glow and other outcome measures.

Amber light sources may not be an ecological panacea

Our results indicate that DE Amber and PC Amber LED light sources may be useful for the reduction of relative sky glow, but there has been limited study on the impacts of amber ALAN on wildlife at typical outdoor illuminance/irradiance levels. Some ecologists postulate that light sources with reduced or no short wavelength content may be less harmful to wildlife than commercially available PC white LED sources with CCTs of 3000 K and higher (Gaston et al. 2013; Longcore et al. 2018), though it is widely understood that any prescription is taxonomically dependent. Many ALAN field studies examine the effect of just one or a few doses of nominally white or broadband ALAN (Newport et al. 2014), rather than evaluating dose-responses under narrowband spectra. Thus far, there are few published studies using amber radiation to examine direct or indirect taxonomical effects, and more are needed to understand if meaningful doses of short-wavelength-depleted light sources are harmful compared to otherwise dark nights.

Table 6 Specification structure for categorizing the chromaticity of light sources relative to the ANSI quadrangles.

Category	Basis	Specification	Impact on Relative Sky Glow (RSG)
Target CCTs from 2200 K to 6500 K	*Basic* or *Extended* Quadrangles from ANSI C78.377-2017	"Categorical CCT" Example: "3500 K", "2200 K", etc.	Higher RSG than high pressure sodium (HPS)
Target CCTs of 2000 K and 1800 K	*Expanded Basic* or *Expanded Extended* Quadrangles from **Table 2**	"Categorical CCT" Example: "2000 K" or "1800 K"	Many SPDs will have lower RSG than HPS, especially those with less short wavelength emission
PC Amber *(PC Amber implies an SPD with a broadband spectral component generated by a reddish phosphor and may have a noticeable short wavelength "hump")*	Chromaticity tolerance specified in **Table 3**	When there is no overlap with *Expanded* Quadrangles: "PC Amber" When there is overlap with one of the *Expanded* quadrangles: "PC Amber – 2000 K" Or "PC Amber – 1800 K"	All likely variations of PC Amber will have lower RSG than HPS
DE Amber *(DE Amber LEDs are narrowband with a peak wavelength near approximately 590 nm. They emit light directly—they do not use phosphor—and have no broadband spectral component.)*	Color Name & Peak Wavelength	"DE Amber – Peak WL nm" Example: "DE Amber – 590 nm"	All variations of DE Amber will have lower RSG than HPS
Other narrowband DE LEDs *(SPDs with chromaticities near the spectrum locus and peak wavelengths longer than approximately 595 nm)*	Color Name & Peak Wavelength	"DE Color Name – Peak WL nm" Example: "DE Red – 640 nm"	Lowest RSG; lower RSG than DE Amber

Early evidence suggests that amber radiation at night may have negative consequences. Some vertebrates (including chickens, salamander, goldfish) and invertebrates (including bees, elephant hawk moths, Tau emerald dragonflies, Asian swallowtail butterflies, and nocturnal spiders) have medium- and/or long-wavelength photoreceptors that are sensitive to amber and/or red light (Menzel and Blakers 1976; Hart 2001; Falcón et al. 2020).

In several studies, amber sources were less disruptive to birds, insects, and marine taxa than white sources—albeit with some species-specific exceptions—though they still had measurable impact. Aulsebrook et al. (2020a; 2020b) found that both amber and white anthropogenic light at night (ALAN) disrupted sleep in domestic pigeons and black swans, though the amber ALAN was less disruptive than white ALAN for magpies. Deichmann et al. (2021) found that in a tropical forest, in general, insects were least attracted to "Amber" (filtered PC White with a CCT of 3000 K) light traps, compared to unfiltered 3000 K traps, but "Amber" was the most attractive for some groups of bioluminescent insects, including elaterid beetles (click beetles) and mycetophilid flies (fungus flies). Owens and Lewis (2021) found that bright "amber" light, with a peak wavelength of 613 nm, disrupted firefly courtship more than blue or red light, with male fireflies exhibiting the fewest flash patterns, and female fireflies not flashing at all under this spectrum and intensity (a negative impact since fireflies use light flashes to communicate).

Plants use optical radiation between 400 and 700 nm to conduct photosynthesis and optical radiation between 530 and 700 nm also contributes to secondary metabolism, photoperiodic, and shade avoidance responses (IES 2021b). Although a lack of studies exists here also with regards to amber LED light at night and plant responses, LPS and HPS sources both have sufficient long-wavelength light to induce photoperiodic responses (Bennie et al. 2016). Urban ALAN is associated with earlier tree flowering (ffrench-Constant et al. 2016; Zheng et al. 2021) and HPS street lighting adjacent to field crops can delay soybean flowering (Palmer et al. 2017).

Finally, scientists are not immune to the lack of clarity brought about by a lack of standardized terminology. Several of the referenced "amber" light sources mentioned above would not be classified as PC Amber nor DE Amber using the specification structure in **Table 6**. One light source from Owens and Lewis (2021) is closer to orange or orange-red, with a peak wavelength of 613 nm; the other from Deichmann et al. (2021) is close to yellow, at least according to the Society of Automotive Engineers.

5. Conclusion

The color appearance of light in the outdoor nighttime environment is most commonly specified using categorical CCT from the CCT quadrangles of ANSI C78.377-2017(NEMA 2017), which do not include CCT categories below 2200 K. Importantly, however, products with CCTs lower than 2200 K and outside of the ANSI designation are being developed by lighting manufacturers and used by lighting specifiers as a strategy to reduce the negative ecological impacts of light at night. In this work we have *Expanded* the *Basic* and *Extended* ANSI quadrangles to include target CCTs of 2000 K and 1800 K and provided designations for specifying phosphor-converted (PC) and direct-emission (DE) Amber LEDs. These specifications provide a uniform specification structure for general illumination light sources not currently included in standardized chromaticity ranges or specifications. These specifications are simple and provide a parsimonious method for reducing the portion of relative sky glow related to light source spectral power distribution. For this reason, we encourage lighting standards development organizations to take up the work of standardizing designations for non-white light sources in the outdoor nighttime environment to increase the clarity of lighting specification.

Funding

This work was funded by Efficiency Forward, Inc., parent company to the DesignLights Consortium.

Disclosure Statement

TE was compensated by Efficiency Forward for work on this project. LR is an employee of DesignLights Consortium. The DesignLights Consortium is a non-profit organization that relies on revenue from its programs to fund its operations. DLC reserves the right to implement programs derived from its research, including this research.

Acknowledgements

We want to gratefully acknowledge the professionals who took the time to share with us their knowledge, experience, and perspectives. Their input was indispensable.

Supplemental Material

An adaptation of the ANSI/IES TM-30-18 Basic Excel calculator was created to help determine the specifications described in **Table 6**. Instructions for use can be found on the "NWL Specification" tab. This calculator is not endorsed by the Illuminating Engineering Society.

References

Anonymized personal communication. 2022. During this work we interviewed six lighting professionals working for different LED chip manufacturers, five professional lighting designers at different firms, four professional lighting researchers at different institutions, and seven professionals that either hold other positions in the lighting industry or straddle industries. Two individuals in the latter category are prominent professional astronomers; one is a chronobiologist; one works at the International Dark Sky Association (IDA); one works for the Florida Fish and Wildlife Commission (FWC). Some of our insights were drawn from these conversations and some data was offered under agreement of confidentiality. As a result, we have chosen here to retain the anonymity of all those we interviewed.

Alcott B. 2005. Jevons' paradox. Ecol Econ. 54(1):9–21. https://doi.org/10.1016/j.ecolecon.2005.03.020

Aubé M, Roby J, Kocifaj M. 2013. Evaluating Potential Spectral Impacts of Various Artificial Lights on Melatonin Suppression, Photosynthesis, and Star Visibility. PLOS ONE. 8(7):e67798. https://doi.org/10.1371/journal.pone.0067798

Aubé M, Simoneau A, Wainscoat R, Nelson L. 2018. Modelling the effects of phosphor converted LED lighting to the night sky of the Haleakala Observatory, Hawaii. Mon Not R Astron Soc. 478(2):1776–1783. https://doi.org/10.1093/mnras/sty1143

Aulsebrook AE, Connelly F, Johnsson RD, Jones TM, Mulder RA, Hall ML, Vyssotski AL, Lesku JA. 2020a. White and Amber Light at Night Disrupt Sleep Physiology in Birds. Curr Biol. 30(18):3657-3663.e5. https://doi.org/10.1016/j.cub.2020.06.085

Aulsebrook AE, Lesku JA, Mulder RA, Goymann W, Vyssotski AL, Jones TM. 2020b. Streetlights Disrupt Night-Time Sleep in Urban Black Swans. Front Ecol Evol. 8:131. https://doi.org/10.3389/fevo.2020.00131

Bailes HJ, Lucas RJ. 2013. Human melanopsin forms a pigment maximally sensitive to blue light (λmax ≈ 479 nm) supporting activation of Gq/11 and Gi/o signalling cascades. Proc R Soc B Biol Sci. 280(1759):20122987. https://doi.org/10.1098/rspb.2012.2987

Bará S, Aubé M, Barentine J, Zamorano J. 2020. Magnitude to luminance conversions and visual brightness of the night sky. Mon Not R Astron Soc. 493(2):2429–2437. https://doi.org/10.1093/mnras/staa323

Bennie J, Davies TW, Cruse D, Gaston KJ. 2016. Ecological effects of artificial light at night on wild plants.Swenson N, editor. J Ecol. 104(3):611–620. https://doi.org/10.1111/1365-2745.12551

Berman SM. 1992. Energy Efficiency Consequences of Scotopic Sensitivity. J Illum Eng Soc. 21(1):3–14. https://doi.org/10.1080/00994480.1992.10747980

Birol F, Keppler JH. 2000. Prices, technology development and the rebound effect. Energy Policy. 28(6):457–469. https://doi.org/10.1016/S0301-4215(00)00020-3

Brown TM, Brainard GC, Cajochen C, Czeisler CA, Hanifin JP, Lockley SW, Lucas RJ, Münch M, O'Hagan JB, Peirson SN, et al. 2022. Recommendations for daytime, evening, and nighttime indoor light exposure to best support physiology, sleep, and wakefulness in healthy adults. PLOS Biol. 20(3):e3001571. https://doi.org/10.1371/journal.pbio.3001571

Cao M, Xu T, Yin D. 2023. Understanding light pollution: Recent advances on its health threats and regulations. J Environ Sci. 127:589–602. https://doi.org/10.1016/j.jes.2022.06.020

CIE, editor. 1995. CIE 13.3-1995. Method of measuring and specifying colour rendering properties of light sources. Austria: Commission internationale de l'éclairage, CIE Central Bureau.

CIE. 1997. CIE 126-1997. Guidelines for minimizing sky glow. Vienna: CIE Central Bureau.

Cinzano P, Falchi F, Elvidge CD. 2001. The first World Atlas of the artificial night sky brightness. Mon Not R Astron Soc. 328(3):689–707. https://doi.org/10.1046/j.1365-8711.2001.04882.x

ffrench-Constant RH, Somers-Yeates R, Bennie J, Economou T, Hodgson D, Spalding A, McGregor PK. 2016. Light pollution is associated with earlier tree budburst across the United Kingdom. Proc R Soc B Biol Sci. 283(1833):20160813. https://doi.org/10.1098/rspb.2016.0813

County of Hawaii. 1983. Hawai'i County Code 1983 (2016 Edition, as Amended). Chapter 14 General Welfare. [Internet]. [place unknown]. https://www.hawaiicounty.gov/our-county/legislative/office-of-the-county-clerk/county-code

Davies TW, Bennie J, Gaston KJ. 2012. Street lighting changes the composition of invertebrate communities. Biol Lett. 8(5):764–767. https://doi.org/10.1098/rsbl.2012.0216

Deichmann JL, Ampudia Gatty C, Andía Navarro JM, Alonso A, Linares-Palomino R, Longcore T. 2021. Reducing the blue spectrum of artificial light at night minimises insect attraction in a tropical lowland forest. Insect Conserv Divers. 14(2):247–259. https://doi.org/10.1111/icad.12479

DesignLights Consortium. 2022. Non-White Light Sources for Nighttime Environments [Internet]. Medford, MA. https://www.designlights.org/wp-

content/uploads/2022/05/DLC_Whitepaper_Non-White-Light-Sources-for-Outdoor-Environments_FINAL_05112022.pdf

Donatello S, Quintero RR, Caldas MG, Wolf O, Van Tichelen P, Van Hoof V, Geerken T. 2018. Revision of the EU Green Public Procurement Criteria for Road Lighting. Technical report and criteria proposal (3rd draft). [Internet]. Seville, Spain: Joint Research Centre (JRC); [accessed 2022 Jul 18]. https://susproc.jrc.ec.europa.eu/product-bureau/sites/default/files/contentype/product_group_documents/1581682046/180322_Lighting_TR_3.0.5_draft_SD_clean.pdf

Falchi F, Cinzano P, Duriscoe D, Kyba CCM, Elvidge CD, Baugh K, Portnov BA, Rybnikova NA, Furgoni R. 2016. The new world atlas of artificial night sky brightness. Sci Adv. 2(6):e1600377. https://doi.org/10.1126/sciadv.1600377

Falchi F, Cinzano P, Elvidge CD, Keith DM, Haim A. 2011. Limiting the impact of light pollution on human health, environment and stellar visibility. J Environ Manage. 92(10):2714–2722. https://doi.org/10.1016/j.jenvman.2011.06.029

Falcón J, Torriglia A, Attia D, Viénot F, Gronfier C, Behar-Cohen F, Martinsons C, Hicks D. 2020. Exposure to Artificial Light at Night and the Consequences for Flora, Fauna, and Ecosystems. Front Neurosci [Internet]. [accessed 2022 Feb 18] 14. https://www.frontiersin.org/article/10.3389/fnins.2020.602796

Florida Fish And Wildlife Conservation Commission. Wildlife Lighting Certification Program. Fla Fish Wildl Conserv Comm [Internet]. [accessed 2022 May 5]. https://myfwc.com/conservation/you-conserve/lighting/criteria/certification/

Galadí-Enríquez D. 2018. Beyond CCT: The spectral index system as a tool for the objective, quantitative characterization of lamps. J Quant Spectrosc Radiat Transf. 206:399–408. https://doi.org/10.1016/j.jqsrt.2017.12.011

Gallaway T, Olsen RN, Mitchell DM. 2010. The economics of global light pollution. Ecol Econ. 69(3):658–665. https://doi.org/10.1016/j.ecolecon.2009.10.003

Gaston KJ, Bennie J, Davies TW, Hopkins J. 2013. The ecological impacts of nighttime light pollution: a mechanistic appraisal: Nighttime light pollution. Biol Rev. 88(4):912–927. https://doi.org/10.1111/brv.12036

Government of Andalusia. 2019. Spectral Index G [Internet]. https://www.juntadeandalucia.es/medioambiente/portal/documents/20151/575112/indexG_descrip.pdf/a6cd028d-1ad9-e5f9-1b4c-6dc653eef75c?t=1555502966000

Grubisic M, Haim A, Bhusal P, Dominoni DM, Gabriel KMA, Jechow A, Kupprat F, Lerner A, Marchant P, Riley W, et al. 2019. Light Pollution, Circadian Photoreception, and Melatonin in Vertebrates. Sustainability. 11(22):6400. https://doi.org/10.3390/su11226400

Hart NS. 2001. The Visual Ecology of Avian Photoreceptors. Prog Retin Eye Res. 20(5):675–703. https://doi.org/10.1016/S1350-9462(01)00009-X

Hartley R, Liebel B. 2020. Joining Forces to Protect the Night from Light Pollution. Int Dark-Sky Assoc [Internet]. [accessed 2022 May 4]. https://www.darksky.org/joining-forces-to-protect-the-night-from-light-pollution/

IES. 2019. ANSI/IES TM-30-20. TECHNICAL MEMORANDUM: IES METHOD FOR EVALUATING LIGHT SOURCE COLOR RENDITION. New York, NY: Illuminating Engineering Society.

IES. 2021a. ANSI/IES LS-1-21, Lighting Science: Nomenclature and Definitions for Illuminating Engineering. Illum Eng Soc [Internet]. https://www.ies.org/standards/definitions/

IES. 2021b. ANSI/IES RP-45-21. RECOMMENDED PRACTICE: HORTICULTURAL LIGHTING. New York, NY: Illuminating Engineering Society.

Institute of Astrophysics of the Canary Islands (IAC). 2022. Technical Specifications Catalog V1.5-2022 [Internet]. [accessed 2022 Jul 18]. https://www.iac.es/system/files/documents/2022-05/CATALOGO%20DE%20ESPECIFICACIONES%20T%C3%89CNICAS%20PARA%20LAS%20INSTALACIONES%20DE%20ALUMBRADO%20EXTERIOR%202022-05-05_V1_5.pdf

International Dark-Sky Association (IDA). 2015. New IDA LED Lighting Practical Guide. Int Dark-Sky Assoc [Internet]. [accessed 2022 May 5]. https://www.darksky.org/the-promise-and-challenges-of-led-lighting-a-practical-guide/

International Dark-Sky Association (IDA). 2021. Fixture Seal of Approval Application. Int Dark-Sky Assoc [Internet]. [accessed 2022 May 5]. https://www.darksky.org/our-work/lighting/lighting-for-industry/fsa/apply-fsa/

Joint Industry and Traffic Engineering Council Committee. 2005. Vehicle traffic control signal heads: light emitting diode (LED) circular signal supplement. June 27, 2005. Washington, DC: Institute of Transportation Engineers.

Kinzey BR, Perrin TE, Miller NJ, Kocifaj M, Aube M, Lamphar HA. 2017. An Investigation of LED Street Lighting's Impact on Sky Glow [Internet]. Richland, WA: Pacific Northwest National Lab. (PNNL), Richland, WA (United States); [accessed 2022 Feb 18]. https://doi.org/10.2172/1418092

Kühne JL, van Grunsven RHA, Jechow A, Hölker F. 2021. Impact of Different Wavelengths of Artificial Light at Night on Phototaxis in Aquatic Insects. Integr Comp Biol. 61(3):1182–1190. https://doi.org/10.1093/icb/icab149

Kyba CCM, Kuester T, Sánchez de Miguel A, Baugh K, Jechow A, Hölker F, Bennie J, Elvidge CD, Gaston KJ, Guanter L. 2017. Artificially lit surface of Earth at night increasing in radiance and extent. Sci Adv. 3(11):e1701528. https://doi.org/10.1126/sciadv.1701528

Lewis SM, Wong CH, Owens ACS, Fallon C, Jepsen S, Thancharoen A, Wu C, De Cock R, Novák M, López-Palafox T, et al. 2020. A Global Perspective on Firefly Extinction Threats. BioScience. 70(2):157–167. https://doi.org/10.1093/biosci/biz157

Longcore T, Rodríguez A, Witherington B, Penniman JF, Herf L, Herf M. 2018. Rapid assessment of lamp spectrum to quantify ecological effects of light at night. J Exp Zool Part Ecol Integr Physiol. 329(8–9):511–521. https://doi.org/10.1002/jez.2184

Luginbuhl CB, Boley PA, Davis DR. 2014. The impact of light source spectral power distribution on sky glow. J Quant Spectrosc Radiat Transf. 139:21–26. https://doi.org/10.1016/j.jqsrt.2013.12.004

MacAdam DL. 1942. Visual Sensitivities to Color Differences in Daylight*. JOSA. 32(5):247–274. https://doi.org/10.1364/JOSA.32.000247

MacAdam DL. 1943. Specification of Small Chromaticity Differences*†. JOSA. 33(1):18–26. https://doi.org/10.1364/JOSA.33.000018

MacAdam DL. 1985. Color Measurement: Theme and Variations [Internet]. 2nd ed. Berlin, Germany: Springer Berlin, Heidelberg; [accessed 2022 May 4]. https://doi.org/10.1007/978-3-540-38681-0

Menzel R, Blakers M. 1976. Colour receptors in the bee eye — Morphology and spectral sensitivity. J Comp Physiol. 108(1):11–13. https://doi.org/10.1007/BF00625437

Mueller-Mach R, Mueller GO, Krames MR, Shchekin OB, Schmidt PJ, Bechtel H, Chen C-H, Steigelmann O. 2009. All-nitride monochromatic amber-emitting phosphor-converted light-emitting diodes. Phys Status Solidi RRL – Rapid Res Lett. 3(7–8):215–217. https://doi.org/10.1002/pssr.200903188

NEMA. 2017. ANSI/NEMA C78.377-2017 American National Standard for Electric Lamps-Specifications for the Chromaticity of Solid-State Lighting Products. Rosslyn, VA: National Electrical Manufacturers Association.

Newport J, Shorthouse DJ, Manning AD. 2014. The effects of light and noise from urban development on biodiversity: Implications for protected areas in Australia. Ecol Manag Restor. 15(3):204–214. https://doi.org/10.1111/emr.12120

Owens ACS, Cochard P, Durrant J, Farnworth B, Perkin EK, Seymoure B. 2020. Light pollution is a driver of insect declines. Biol Conserv. 241:108259. https://doi.org/10.1016/j.biocon.2019.108259

Owens ACS, Lewis SM. 2021. Narrow-spectrum artificial light silences female fireflies (Coleoptera: Lampyridae). Insect Conserv Divers. 14(2):199–210. https://doi.org/10.1111/icad.12487

Pacific Northwest National Laboratory (PNNL). Sky Glow Comparison Tool Version 1.0. PNNL-SA-138348 [Internet]. [accessed 2022 Apr 25]. https://www.energy.gov/eere/ssl/potential-impacts-led-street-lighting-sky-glow

Palmer M, Gibbons R, Bhagavathula R, Holshouser D, Davidson D. 2017. ROADWAY LIGHTING'S IMPACT ON ALTERING SOYBEAN GROWTH: VOLUME 1 [Internet]. Springfield, Illinois: Illinois Center for Transportation. https://apps.ict.illinois.edu/projects/getfile.asp?id=5252

Republic of Chile. 2013. DECREE 43 ESTABLISHES EMISSION STANDARD FOR THE REGULATION OF LIGHT POLLUTION. www.bcn.cl/leychile [Internet]. [accessed 2022 Aug 8]. https://www.bcn.cl/leychile/navegar?idNorma=1050704

Republic of Chile. 2021. PRELIMINARY DRAFT EXCERPT OF EMISSION STANDARD PREPARED BASED ON THE REVISION OF SUPREME DECREE NO. 43, OF 2012, OF THE MINISTRY OF THE ENVIRONMENT , WHICH ESTABLISHES EMISSION STANDARD FOR THE REGULATION OF LIGHT POLLUTION. Bibl Congr Nac Chile [Internet]. [accessed 2022

Aug 8].
https://www.diariooficial.interior.gob.cl/publicaciones/2021/04/23/42937/01/1931444.pdf

Rich C, Longcore T, editors. 2006. Ecological consequences of artificial night lighting. Washington, DC: Island Press.

Sánchez de Miguel A, Bennie J, Rosenfeld E, Dzurjak S, Gaston KJ. 2021. First Estimation of Global Trends in Nocturnal Power Emissions Reveals Acceleration of Light Pollution. Remote Sens. 13(16):3311. https://doi.org/10.3390/rs13163311

Sanders D, Frago E, Kehoe R, Patterson C, Gaston KJ. 2021. A meta-analysis of biological impacts of artificial light at night. Nat Ecol Evol. 5(1):74–81. https://doi.org/10.1038/s41559-020-01322-x

Smart Outdoor Lighting Alliance (SOLA). 2017. Community Friendly Lighting Program. Smart Outdoor Light Alliance [Internet]. [accessed 2022 May 5]. https://volt.org/cfl/

Society of Automotive Engineers. 2020. SAE J578 APR2020 (R) Chromaticity Requirements for Ground Vehicle Lamps and Lighting Equipment. Warrendale, PA: SAE International.

Tsao JY, Waide P. 2013. The World's Appetite for Light: Empirical Data and Trends Spanning Three Centuries and Six Continents. LEUKOS. 6(4):259–281. https://doi.org/10.1582/LEUKOS.2010.06.04001

Zheng Q, Teo HC, Koh LP. 2021. Artificial Light at Night Advances Spring Phenology in the United States. Remote Sens. 13(3):399. https://doi.org/10.3390/rs13030399

Zukauskas A, Vaicekauskas R, Tuzikas A, Petrulis A, Stanikunas R, Svegzda A, Eidikas P, Vitta P. 2014. Firelight LED Source: Toward a Balanced Approach to the Performance of Solid-State Lighting for Outdoor Environments. IEEE Photonics J. 6(3):1–16. https://doi.org/10.1109/JPHOT.2014.2319102